8. SCHULZ-FLORY LIMITATIONS

Reactions of syngas (CO/H_2) over a majority of synfuel catalysts, including the conventional Fischer-Tropsch (F-T) catalysts, are nonselective, resulting in products over a broad molecular weight range. Curve-fitting these products with a polymerization model known as the Schulz-Flory (S-F) equation (53,54,55) is often used to classify catalysts (by their S-F compliance versus noncompliance).

Where demands exist for a broad range of products, the use of S-F-compliant catalysts is acceptable. An example of such a marketplace is South Africa, where the SASOL plants have been in operation for some time. In today's market, however, the SASOL situation is considered an exception rather than a trend-setting option. Economic factors favor the use of non-S-F-compliant catalysts in the majority of market situations. This is the driving force for a large number of catalyst development activities for synfuel.

This chapter presents the background of the syngas reaction chemistry and discusses progress toward exceeding the S-F product distribution.

8.1 SCHULZ-FLORY DISTRIBUTION

The S-F polymerization describes a nonselective polymerization of surface species by the addition of carbon units, one at a time, onto the terminal end of a growing chain. One polymer molecule is produced from each chain by the addition of the last carbon unit (53). In each stage of the polymerization process, it is assumed that each surface species has an equal opportunity to react, irrespective of the size. Under these assumptions, the mole fraction of a product having n carbons (M_n) is given by:

$$M_n = (1-P)\, P^{n-1} \qquad (8.1)$$

P is the chain growth probability factor, defined as:

$$P = \gamma_p/(\gamma_p + \gamma_t) \qquad (8.2)$$

γ_p and γ_t ar the rates of propagation and termination, respectively.

Assuming that each carbon unit in the chain is the same weight regardless of its position in the chain, which is a good assumption for paraffinic or olefinic hydrocarbons, Equation 8.1 can be expressed in terms of weight fraction. This is done by multiplying M_n by n and dividing it by 1/(1-P), the average degree of polymerization. The resulting expression for weight fraction is:

$$W_n = n\,(1-P)^2\, P^{n-1} \qquad (8.3)$$

This is usually expressed in the logarithmic form:

$$\log \frac{W_n}{n} = n \log P + \log \frac{(1-P)^2}{P} \qquad (8.4)$$

Data for such a polymerization process fall on a straight line for a plot of log (W_n/n) versus n. The calculated value of P from the slope (log P) and from the intercept (log $[(1-P)^2/P]$) should be consistent.

A degree of polymerization can be defined as:

$$D = \frac{1}{1/(1-P)} \qquad (8.5)$$

From Equation 8.2, D can be expressed as:

$$D = \frac{\gamma_p + \gamma_t}{\gamma_t} \qquad (8.6)$$

At a low degree of polymerization, relatively sharp product distributions are obtained. According to Equation 8.6, the distribution is characterized by $\gamma_t > \gamma_p$. Examples are methane and methanol synthesis, in which D approaches unity. As the degree of polymerization increases, the product distribution becomes broader.

Table 8-1 presents the product distributions for various values of D as calculated by the use of both Equations 8.3 and 8.6. After smoothing out the step values, these data are plotted in Figures 8-1 and 8-2. It can be seen that the most abundant components are those where $n \cong D$. For example, at $D = 6$, $n = 5$ and $n = 6$ are the most abundant; at $D = 20$, $n = 19$ and $n = 20$ are the most abundant.

A striking fact about the product distribution is the sharp drop in the weight percent of the most abundant components as the value of D increases (Figure 8-3). In fact, the distinction between the most abundant components and their neighboring components becomes less conspicuous as D increases above ~8.

Because of the broad product distribution, at each value of D there are likely to be substantial yields of gas (C_1-C_4), gasoline (C_5-C_{11}), diesel (C_{12}-C_{25}), and heavies (C_{25}+). Figure 8-4 gives another representation of Table 8-1 in terms of these product fractions. It is useful to identify specific D values for maximizing a desired product cut. Figure 8-4 also illustrates the fact that some product optimization is possible within the S-F reactions. Whether this yield control is enough to justify a plant based on the S-F reaction schemes is an economic matter that must be evaluted for each market situation.

The test data obey the correlations predicted by the S-F polymerization mechanism quite well. For example, Catalytica has compiled various German data and has presented them as S-F plots (23). One such plot is shown in Figure 8-5. The data are from tests using iron catalysts. Despite the fact that catalyst compositions were different and the tests were carried out in different units and at different times, the data points show a remarkable agreement with the S-F correlation.

Table 8-1

Schulz-Flory Distribution of Component Carbon Number, n, at Each Degree of Polymerization, D

n \ D	1	2	3	4	6	8	10	12	14	16	18	20
1	100	25.0	11.1	6.3	2.8	1.6	1.0	0.7	0.5	0.4	0.3	0.3
2		25.0	14.8	9.4	4.6	2.7	1.8	1.3	0.9	0.7	0.6	0.5
3		18.8	14.8	10.5	5.8	3.6	2.4	1.8	1.3	1.0	0.8	0.7
4		12.5	13.2	10.5	6.4	4.2	2.9	2.1	1.6	1.3	1.0	0.9
5		7.8	11.0	9.9	6.7	4.6	3.3	2.5	1.9	1.5	1.2	1.0
6		4.7	8.8	8.9	6.7	4.8	3.5	2.7	2.1	1.7	1.4	1.2
7		2.7	6.8	7.8	6.5	4.9	3.7	2.9	2.3	1.9	1.5	1.3
8		1.6	5.2	6.7	6.2	4.9	3.8	3.0	2.4	2.0	1.7	1.4
9		0.9	3.9	5.6	5.8	4.8	3.9	3.1	2.5	2.1	1.8	1.5
10		0.5	2.9	4.7	5.3	4.7	3.9	3.2	2.6	2.2	1.8	1.6
11		0.3	2.1	3.9	4.9	4.5	3.8	3.2	2.7	2.3	1.9	1.6
12		0.2	1.5	3.2	4.5	4.3	3.8	3.2	2.7	2.3	2.0	1.7
13			1.1	2.6	4.1	4.1	3.7	3.2	2.7	2.3	2.0	1.7
14			0.8	2.1	3.6	3.9	3.6	3.1	2.7	2.4	2.1	1.7
15			0.6	1.7	3.2	3.6	3.4	3.1	2.7	2.4	2.1	1.8
16			0.4	1.3	2.9	3.4	3.3	3.0	2.7	2.4	2.1	1.8
17			0.3	1.1	2.6	3.1	3.2	2.9	2.7	2.4	2.1	1.9
18			0.2	0.8	2.3	2.9	3.0	2.8	2.6	2.3	2.1	1.9
19				0.7	2.0	2.7	2.9	2.8	2.6	2.3	2.1	1.9
20				0.5	1.7	2.5	2.7	2.7	2.5	2.3	2.1	1.9
21				0.4	1.5	2.3	2.6	2.6	2.4	2.2	2.1	1.88
22					1.3	2.1	2.4	2.5	2.3	2.22	2.04	1.87
23					1.2	1.9	2.3	2.4	2.3	2.17	2.02	1.86
24					1.0	1.7	2.1	2.3	2.2	2.12	1.99	1.84
25					0.9	1.6	2.0	2.15	2.15	2.07	1.96	1.82
26					0.8	1.4	1.9	2.05	2.08	2.02	1.92	1.80
27					0.7	1.3	1.74	1.95	2.01	1.97	1.89	1.78
28					0.6	1.2	1.63	1.86	1.93	1.91	1.85	1.75
29					0.5	1.1	1.52	1.76	1.80	1.86	1.81	1.72
30					0.4	9.8	1.41	1.67	1.78	1.80	1.76	1.69

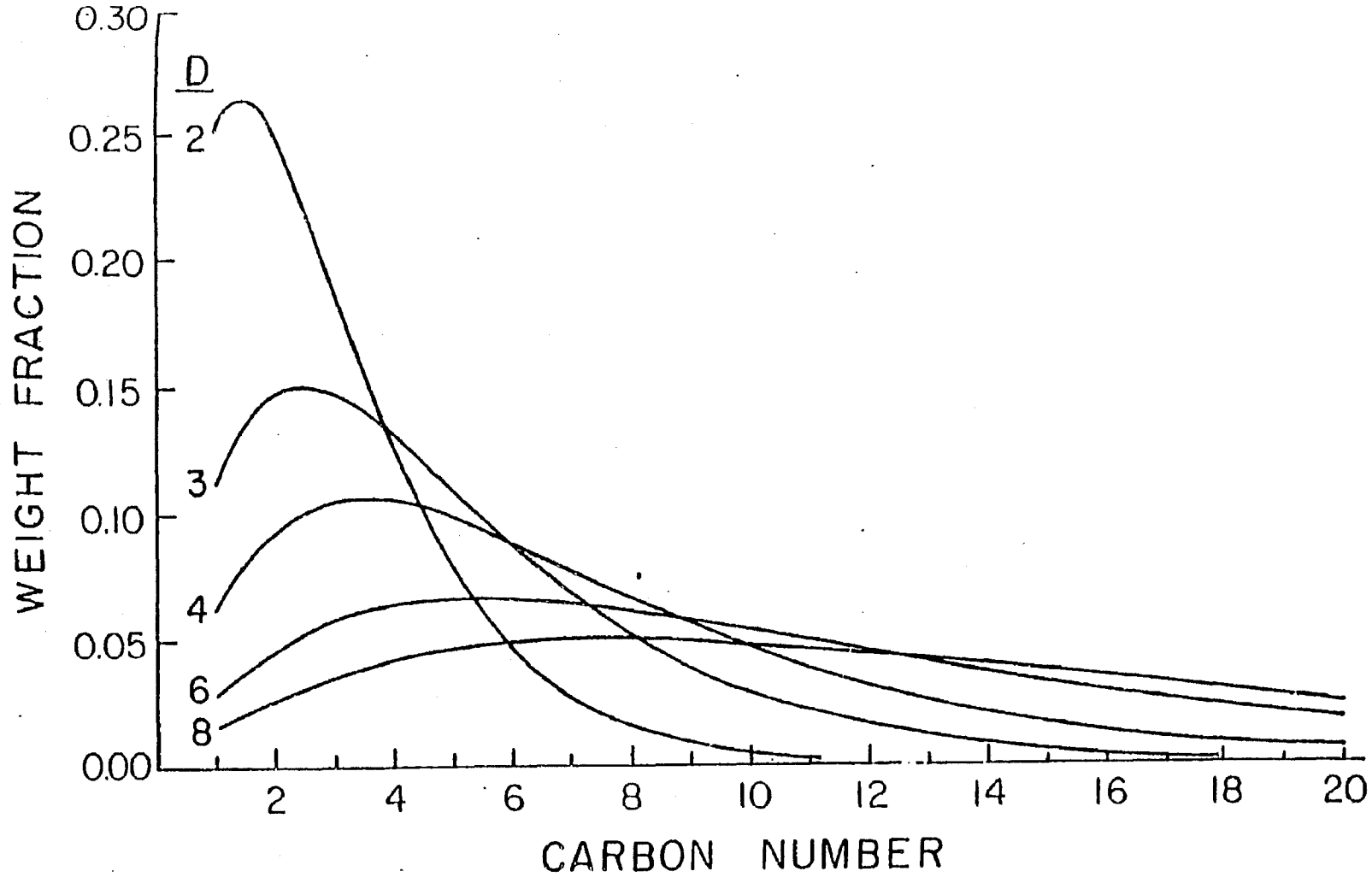

Figure 8-1. Hydrocarbon Distribution from Schulz-Flory Polymerization (Degree of Polymerizatin from 2 to 8)

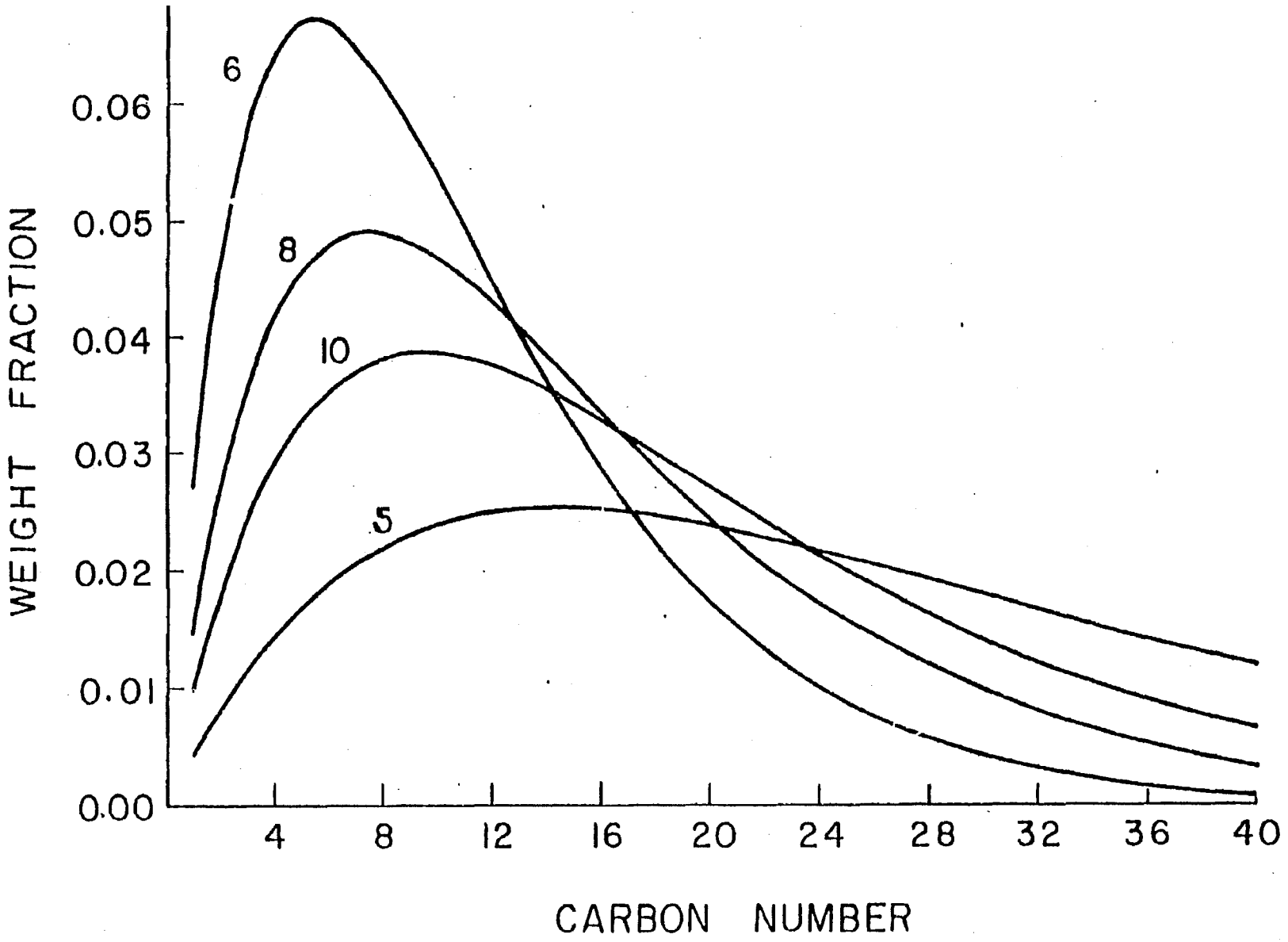

Figure 8-2. Hydrocarbon Distribution from Schulz-Flory Polymerization (Degree of Polymerization from 6 to 15)

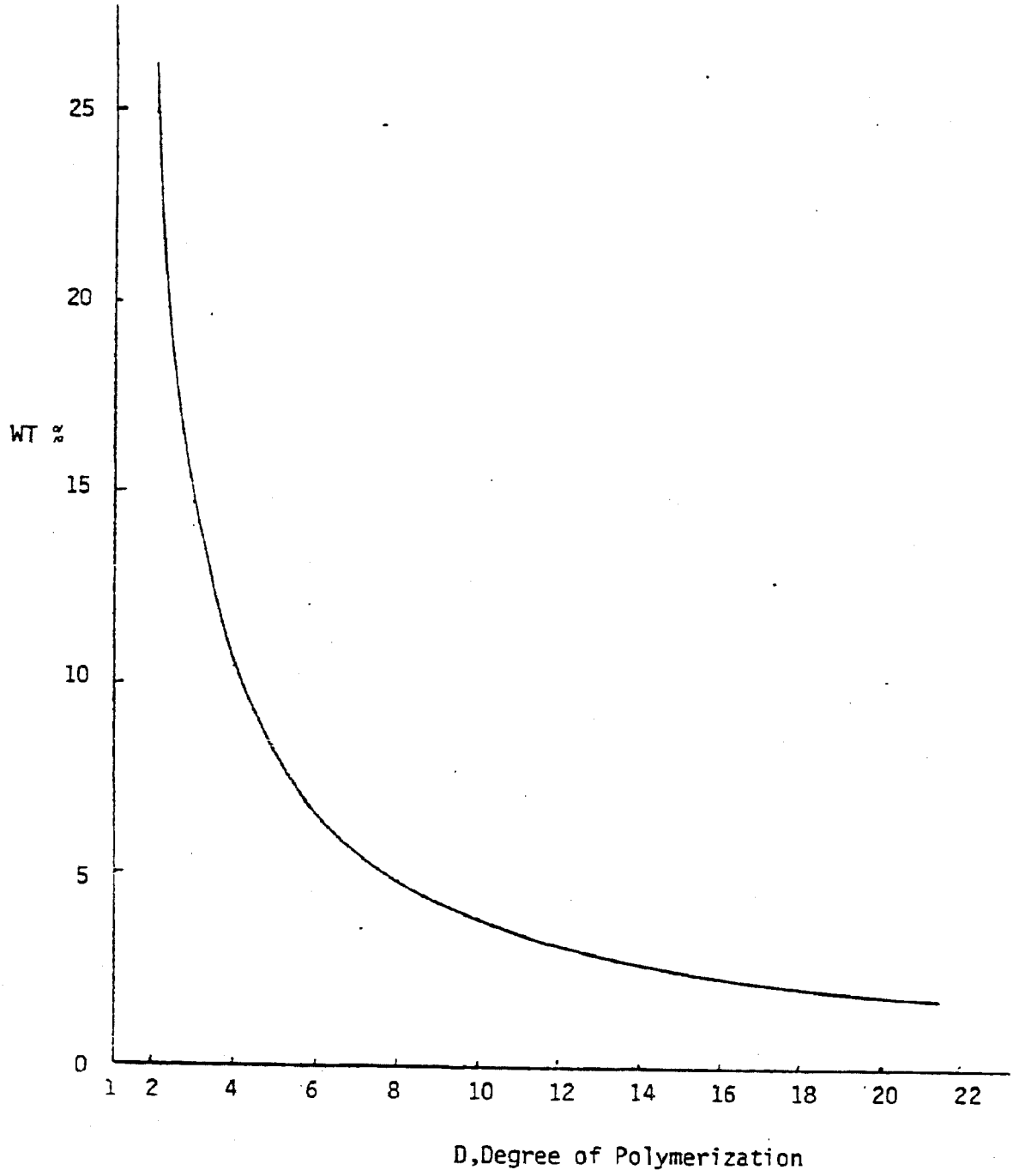

Figure 8-3. Schulz-Flory Distribution: Weight Percent of Most Abundant Components at Each D Value

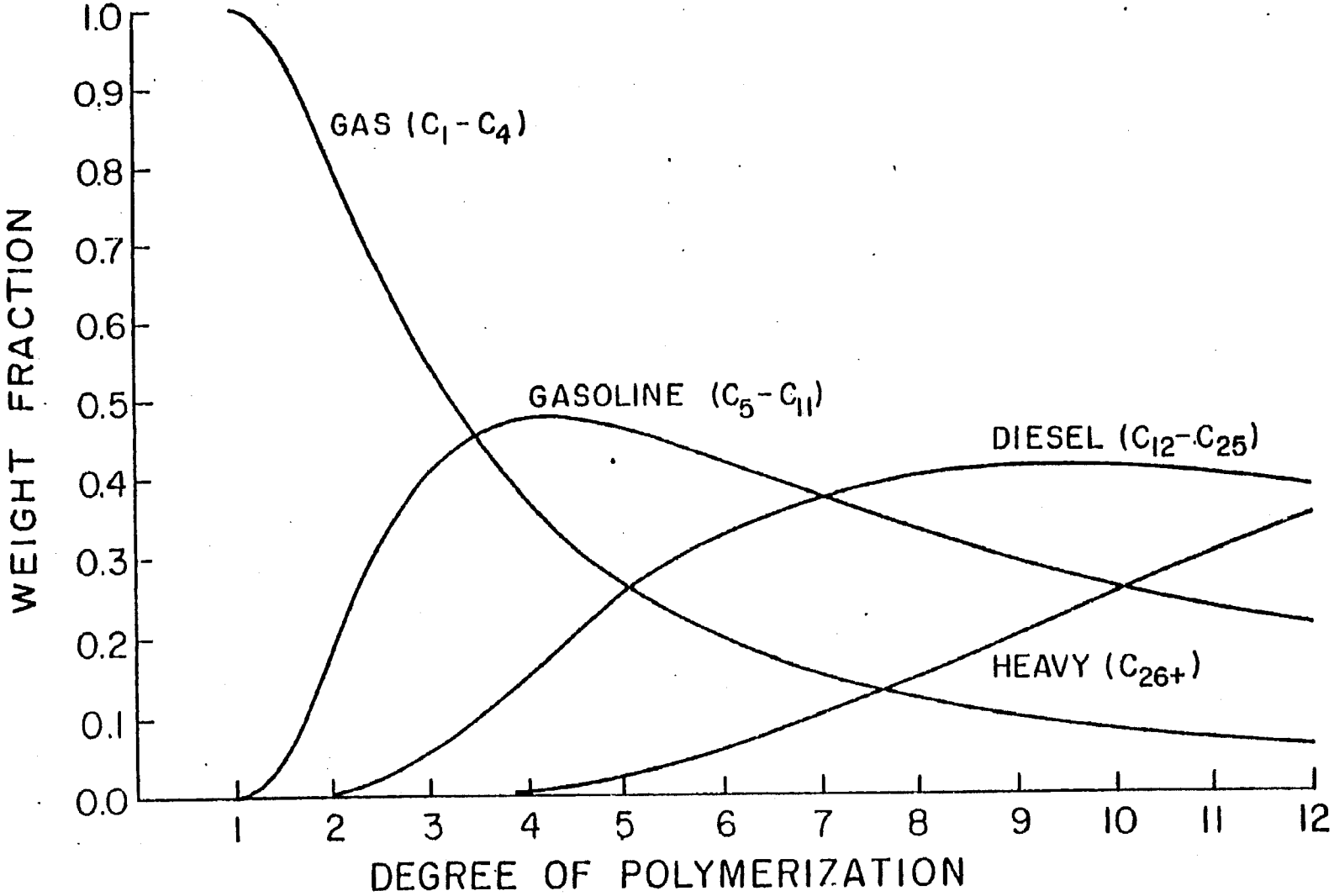

Figure 8-4. Variation of Typical Product Split with Degree of Polymerization

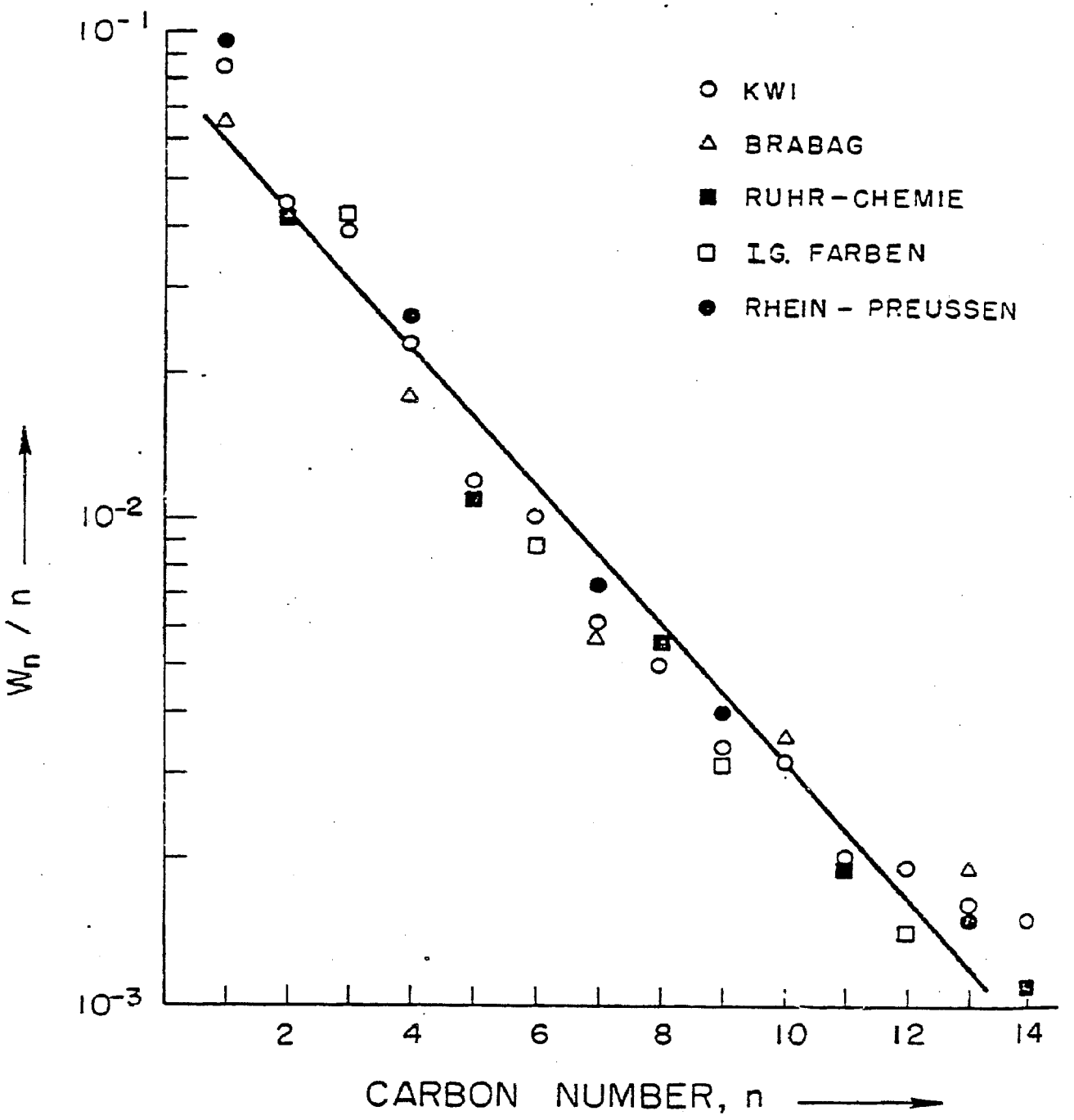

Figure 8-5. Hydrocarbon Product Distribution for Iron Catalysts. Data from KWI, Brabag, Ruhrchemie, I. G. Farben, and Rhein-Pressen plotted according to Equation 8.4

Reference: (23, 57)

Table 8-2

Product Distribution of F-T Reactions Over Co Catalyst

Carbon No.	Wt % of Total Hydrocarbons
1	15.0
2	1.3
3	4.0
4	7.4
5	10.0
6	10.2
7	8.3
8	6.2
9	5.0
10	4.2
11	3.3
12	2.9
13	2.4
	80.2

Reference: (23, 56)

Some discrepancies occur in the S-F correlation when Co is the catalyst. The results of Pichler (23,56), as an example, are tabulated in Table 8-2. Note that the products add up to 80%, which indicates the presence of unlisted $C_{14}+$ products. A plot of weight percent distribution versus carbon number is shown in Figure 8-6. An abnormal dip for C_2, C_3, and C_4, and excess C_1 are evident from the plot. Figure 8-7 is a S-F plot of the data. The deviations for C_1, C_2, C_3, and C_4 are clearly shown. A good correlation is seen for C_5-C_{13} products. The reason for the deviation is believed to be due to higher hydrogenation and cracking of light olefins by Co, rather than by Fe (23).

8.2 NON-SCHULZ-FLORY DISTRIBUTION

8.2.1 Synfuel Options

There are two basic approaches to increasing the selectivity of synfuel production from syngas beyond what is possible with the S-F reactions. One is represented by Mobil's Methanol-to-Gasoline (MTG) process (Chapter 3), in which syngas is converted to a highly functional intermediate, such as methanol, at a very high selectivity; the intermediate is subsequently converted to the desired synfuel, also at a high selectivity. This approach uses two functionally different catalysts operating under different process conditions. The second approach is represented by Union Carbide's process (Chapter 3) in which a multifunctional catalyst converts syngas to synfuels in one step. This approach has the intrinsic advantage of having a simpler process configuration. This is, however, countered by the requirement of complex catalytic functions.

An intermediate approach is Mobil's MTG process, involving a slurry-phase F-T and a ZSM-5 reactor (86). In this scheme, the aim is to convert syngas from the advanced gasifier (low H_2/CO ratio) to olefins and oxygenates in the slurry-phase F-T reactor. The ZSM-5 reactor then converts the olefins and oxygenates to gasoline, and the heavy fractions to light hydrocarbons. The slurry reactor to be developed for this scheme should be essentially the same as the one for the Union Carbide approach, but the catalytic functions are somewhat different.

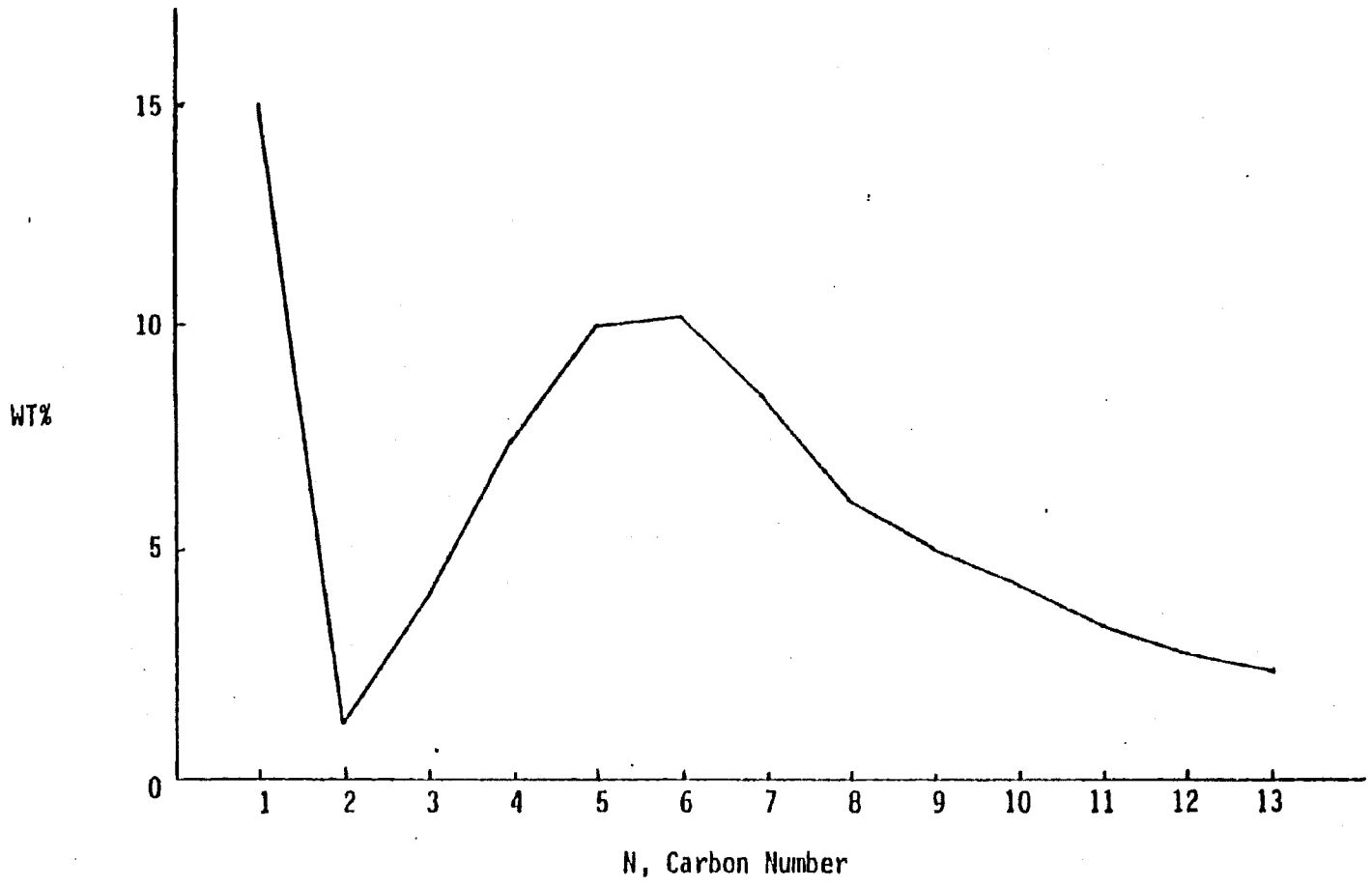

Figure 8-6. Product Distribution of Fischer-Tropsch Reactions Over Co Catalyst

Reference: (56)

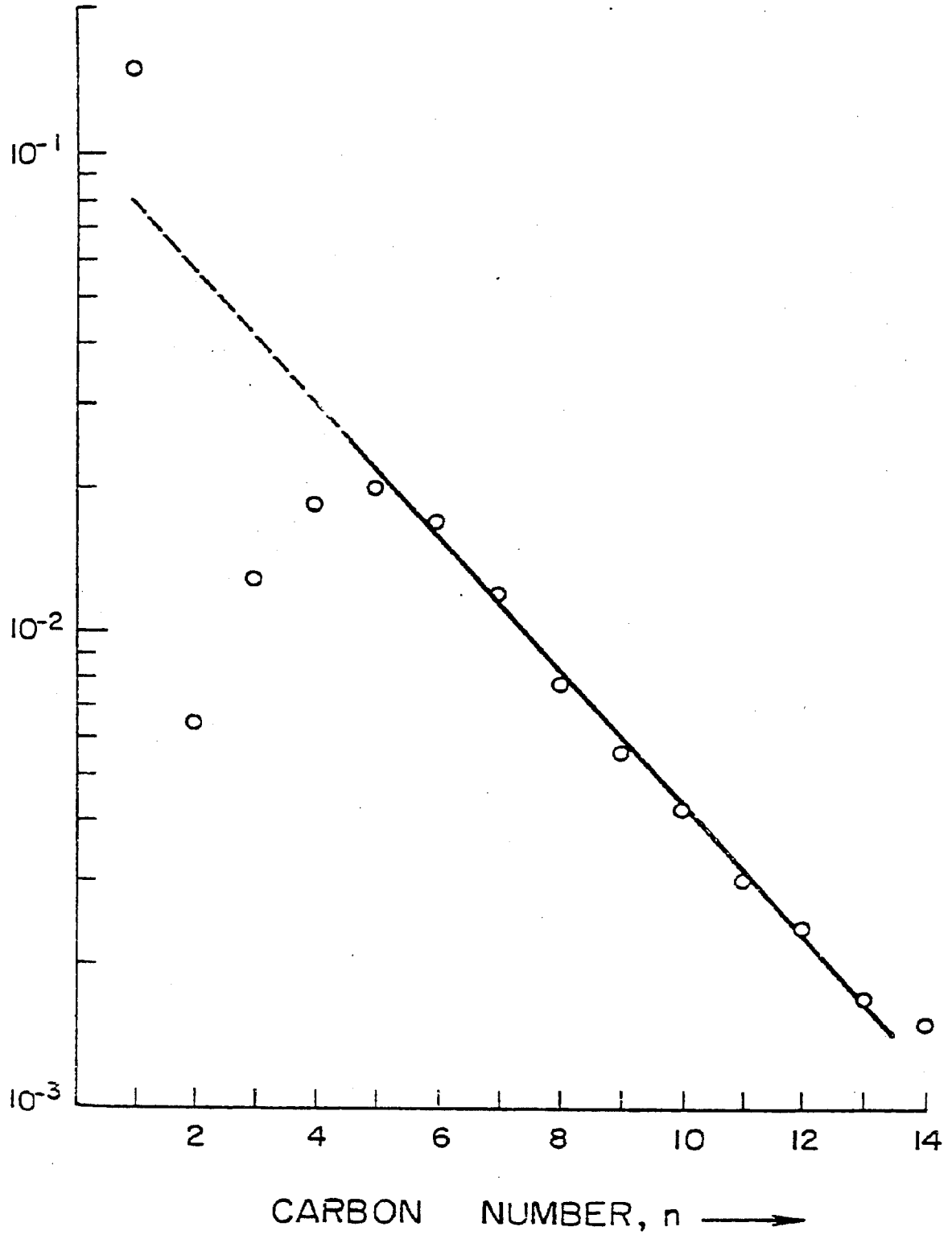

Figure 8-7. Hydrocarbon Product Distribution for a Cobalt Catalyst. Plotted According to Equation 8.4.

Reference: (56)

The development of ZSM-5 catalyst has advanced Mobil's MTG approach to the stage where commercial demonstration is contemplated (58). Challenges remain for the development of the slurry reactor and the catalysts. Some perspectives of catalyst development are provided below.

The near-term options of one-step synfuel production from syngas are summarized in Figure 8-8. The state-of-the-art technologies of SASOL and the options available from second-generation technologies are shown. The advanced options include catalysts capable of higher product selectivities than those predicted by the Schulz-Flory (S-F) model.

The most attractive route would be the combination of an advanced gasifier and slurry-phase synthesis with a S-F bypass catalyst yielding desired products beyond the S-F limitations. There are two critical development hurdles in this route: the development of slurry-phase technology and the development of its catalyst. The challenges in the reactor development are discussed in Chapter 4. Equally challenging is the S-F bypass catalyst for slurry-phase application. This catalyst must possess the following basic capabilities:

- CO shift
- High CO conversion per pass
- Polymerization
- Selective termination of polymerization
- Operation under slurry environment

The S-F bypass catalyst can contribute in the other advanced synfuel options (Figure 8-8). Here, the reaction environment is gaseous, and an external shift is provided.

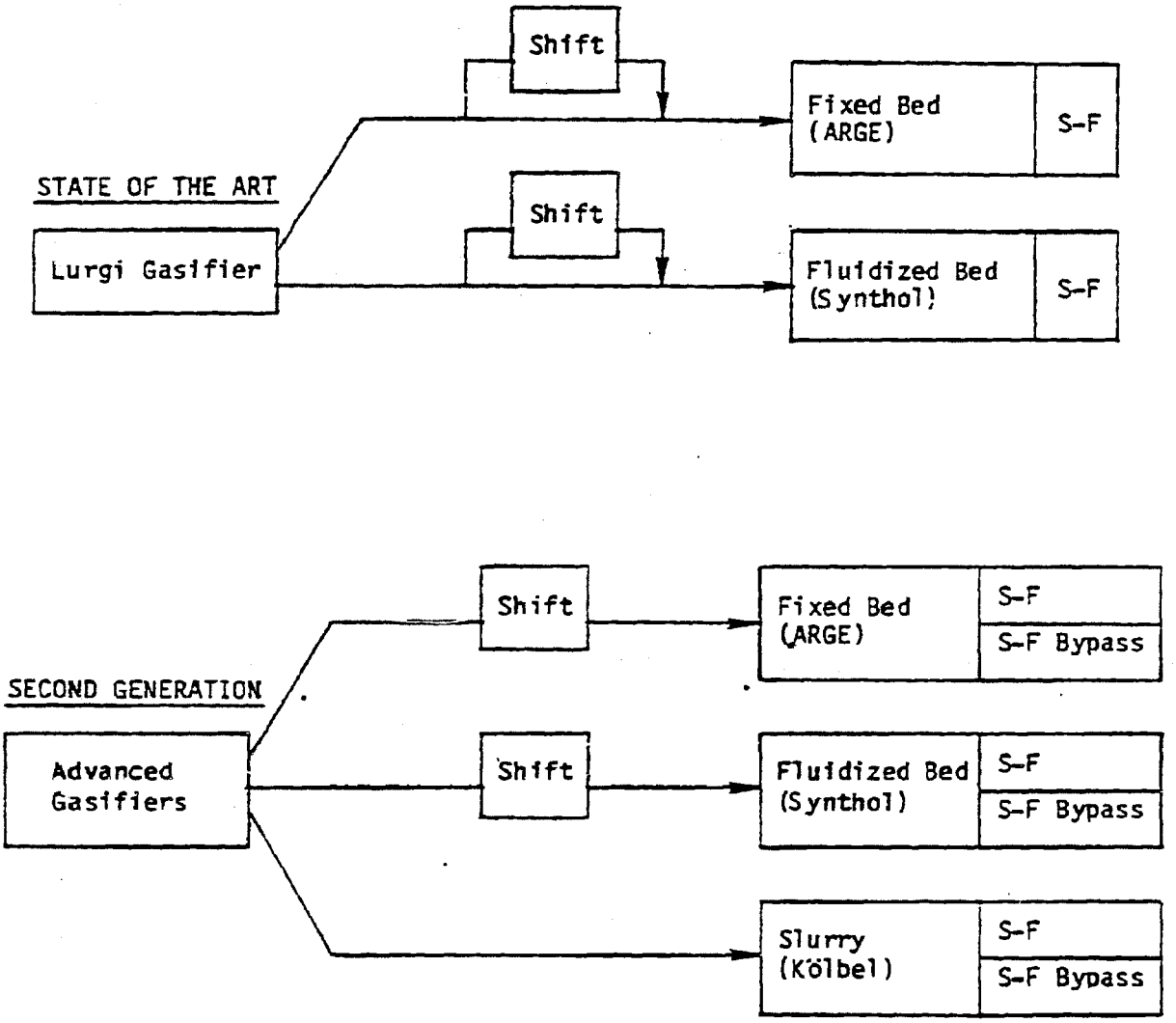

Figure 8-8. One-Step Synfuel Production Options

8.2.2 Chain Reactivity

The basic assumptions used in the derivation of the Schulz-Flory distribution function specify equal reactivity of all surface oligomers and chain growth by addition of one-carbon units. While both of these assumptions are reasonable and the distribution function appears to fit much of the hydrocarbon synthesis data, the assumption of equal oligomers reactivity deserved some discussion.

For long hydrocarbon chains (C_4 and above) the assumption of equal reactivity toward polymerization is probably justified. The rate of polymerization, r_p, and rate of termination, r_t, should be very similar for species of different chain length where the ligands attached to the metal can be viewed as $(CH_2)_n$ groups; hence the metal-carbon bonds are almost identical. For shorter hydrocarbon surface species, such as C_1-C_3, however, the ligand attached to the metal is significantly different; as a consequence, the carbon-metal bond may display some differences resulting in modifications of r_p and r_t. Changes in r_p and r_t affect the probability of polymerization, P, of each oligomer because $P = r_p/(r_p + r_t)$. Thus, deviations from the expected Schulz-Flory distribution of hydrocarbons are most likely to be observed in the C_1-C_4 range if the deviation is due to variation in oligomer reactivity. Although the surface hydrocarbon species mentioned above are alkyl groups, the same arguments would hold for alkyne groups or oxygen-containing species.

8.2.3 Catalyst or Reactor Nonuniformity

Hydrocarbon synthesis catalysts that on a microscopic scale yield a product distribution consistent with Schulz-Flory may, nevertheless, give a product distribution in large-scale reactor tests that is not consistent with the Schulz-Flory distribution. This situation can arise from nonuniformities in the reactor, either from an intrinsically nonuniform catalyst or from varying process conditions within the reactor. The effect of such nonuniformities on the expected product distributions can be readily modeled. Several possible situations are treated in this section.

One occurrence that is frequently encountered in hydrocarbon synthesis tests is the presence of hot spots in the reactor due to the highly exothermic nature of the reaction. With a given catalyst operating under fixed process conditions, an increase in temperature generally results in a shift of the product distribution to lower-molecular-weight hydrocarbons. If it is assumed that the reactor is divided into two regions that are effectively uniform, the product distribution is given by the sum of the distributions produced by each region. Product distributions are then generated by assuming an average degree of polymerization for each catalyst region and the fraction of product contributed by each region.

8.2.4 Product Incorporation in Chain

It is well-known that reactive hydrocarbon species, such as olefins, alcohols, and ketones, are capable of adsorbing and initiating the synthesis of higher hydrocarbons in the presence of CO and H_2 over Fischer-Tropsch catalysts (81,82). Such reactions can lead to alternate mechanistic pathways for hydrocarbon synthesis, in which the reaction of CO and H_2 produces an initial product mixture containing olefins, with a portion of these olefins re-entering the surface reaction.

8.2.5 Production of Oxygen-containing Products

Hydrocarbon synthesis from CO and H_2 can yield alcohols as the final product, depending on catalyst properties and process conditions. The amount of alcohol products can vary from a small fraction to 100% of the synthesis products.

For such cases, product weight fractions, W_n, cannot be used to assess consistency with the Schulz-Flory function because the basic assumption of equal monomer weight is not valid. For product distributions containing alcohol or other oxygenates, the mole fraction expression:

$$M_n = P^{n-1} (1-P) \qquad (8.7)$$

and the logarithmic form:

$$\text{Log } M_n = n \log P + \log\left(\frac{1-P}{P}\right) \tag{8.8}$$

must be used to assess Schulz-Flory behavior. To illustrate this point, an alcohol product distribution (in mole fraction) of each oligomer was generated from Equation 8.7. This distribution is, of course, consistent with the Schulz-Flory polymerization process. This distribution was converted to a weight fraction distribution by multiplying each oligomer mole fraction by the molecular weight of a normal alcohol and normalizing, as expressed in Equation 8.9:

$$W_n \text{ (alcohol)} = \frac{P^{(n-1)}(1-P)(14n + 18)}{\sum_{m=1}^{\infty} P^{(m-1)}(1-P)(14m + 18)} \tag{8.9}$$

Both weight fraction divided by carbon number, W_n/n, and mole fraction, M_n, are graphed in Figure 8-9. As expected, the W_n/n versus n plot shows significant curvature at low carbon number where the effect of the added oxygen is large. Use of mole fraction to test correlation with the Schulz-Flory polymerization process yields a linear plot with a similar probability of polymerization calculated from both the slope and intercept.

8.3 EXPERIMENTAL ARTIFACTS

Obtaining representative product distributions as the reaction is occurring in the reactor is sometimes difficult. This may lead to the wrong interpretation of the catalytic activities. Major causes of such experimental artifacts can often be traced to the following common phenomena:

- Condensation and capillary condensation of products on the catalyst
- Condensation of products in downstream equipment and lines
- Incomplete recovery of products from traps

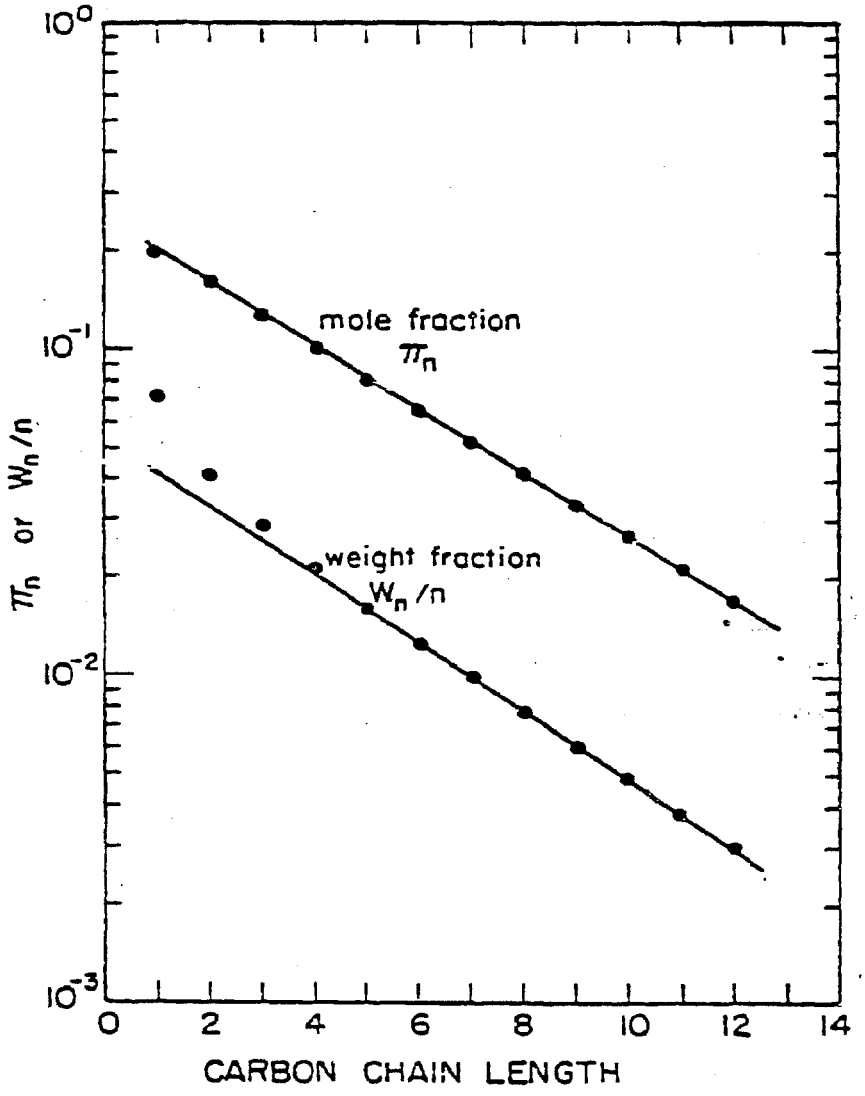

Figure 8-9. Schulz-Flory Alcohol Distribution Plotted as Mole Fraction and Weight Fraction versus Carbon Chain Length. D = 5.

While active researchers are generally aware of such problems, the magnitude of their effects can often be underestimated. This section discusses solutions for these artifacts. More details can be obtained from the literature (75).

8.3.1 Product Condensation in the Reactor

One of the major phenomena that can influence the measured product distribution in an experimental or bench-scale test is condensation of a portion of the products in the reactor. This can occur by three processes:

(1) A portion of the products may be physically and chemically adsorbed on the catalyst surface. This effect would be largest for high-surface-area catalysts and for polar products such as alcohols or olefins. In general, however, the amount of material retained is small because the capacity of even a high-surface-area catalyst is minimal compared to hydrocarbon production, if the reaction period is sufficiently long. For example, a 5% Ru/Al_2O_3 catalyst with a site time yield (turnover frequency) of 0.1 s^{-1} produces 1.5×10^{18} C_5 hydrocarbon molecules per gram of catalyst per second, assuming a Ru dispersion of 25%. This saturates the surface of a 100 m^2/g catalyst, assuming 10^{15} sites per cm^2, in ~10 min. Of course, the actual capacity of such a surface is much less.

(2) Capillary condensation of products in the catalyst pores or condensation of the products in the reactor itself can lead to significant problems because the capacity for this form of holdup could be large. For example, a typical synthesis catalyst, such as precipitated iron or cobalt catalysts, exhibits production rates of 0.01-0.1 g hydrocarbon/g catalyst/h (77). If high-boiling-point products, representing 10-20% of the total products, are retained on the catalyst, the production rate of retained hydrocarbons is 0.001-0.02 g/g cat/h. For a catalyst with a void volume of 0.1-0.3 cm^3/g catalyst, 5-300 h would be required before the voids

are saturated and the high-boiling-point products appear in the product stream.

(3) Low-temperature regions within the reactor or in the product collection system can also lead to alterations in the product distribution due to preferred condensation of low-vapor-pressure species. The material holdup in this case can be as large as that discussed in (2) above.

Product retention, as described above, could significantly alter the product distribution in the early stages of reaction. However, with time the product distribution approaches that produced by the catalyst because the sinks that collect the product hydrocarbons become saturated. For this reason, product distributions obtained after short periods of catalyst operation are more likely to be influenced by physical phenomena. It should also be noted that as the product distribution is approaching a steady-state value, the intrinsic activity and selectivity of the catalyst may change. This aspect makes determination of initial activity and selectivity difficult, especially when the production of higher hydrocarbons is significant.

A condensation model predicts a discrepancy between the measured and actual products, as shown in Figure 8-10, when the reactor produces products of Schulz-Flory (S-T) distribution of D = 10 (degree of polymerization) and allows products to leave the reactor based on the vapor-liquid equilibrium at 200°C. The distinct product distribution, with the peak at C = 9, and rapid falloff in the higher hydrocarbons, is a result of product retention. This effect should decrease as the degree of polymerization is lowered.

When the reaction is run for extended periods, the condensed products saturate the reactor and catalyst voids and flows into the product collection system. The products exiting the reactor begin to approach the distribution produced by the catalyst. Collection of "wax" within the reactor, plugging of the reactor by heavy hydrocarbon products, and the slow transfer of viscous liquid hydrocarbons from the reactor are commonly observed during the synthesis of hydrocarbons over cobalt and iron catalysts (76,77). These effects result in a slow, asymptotic

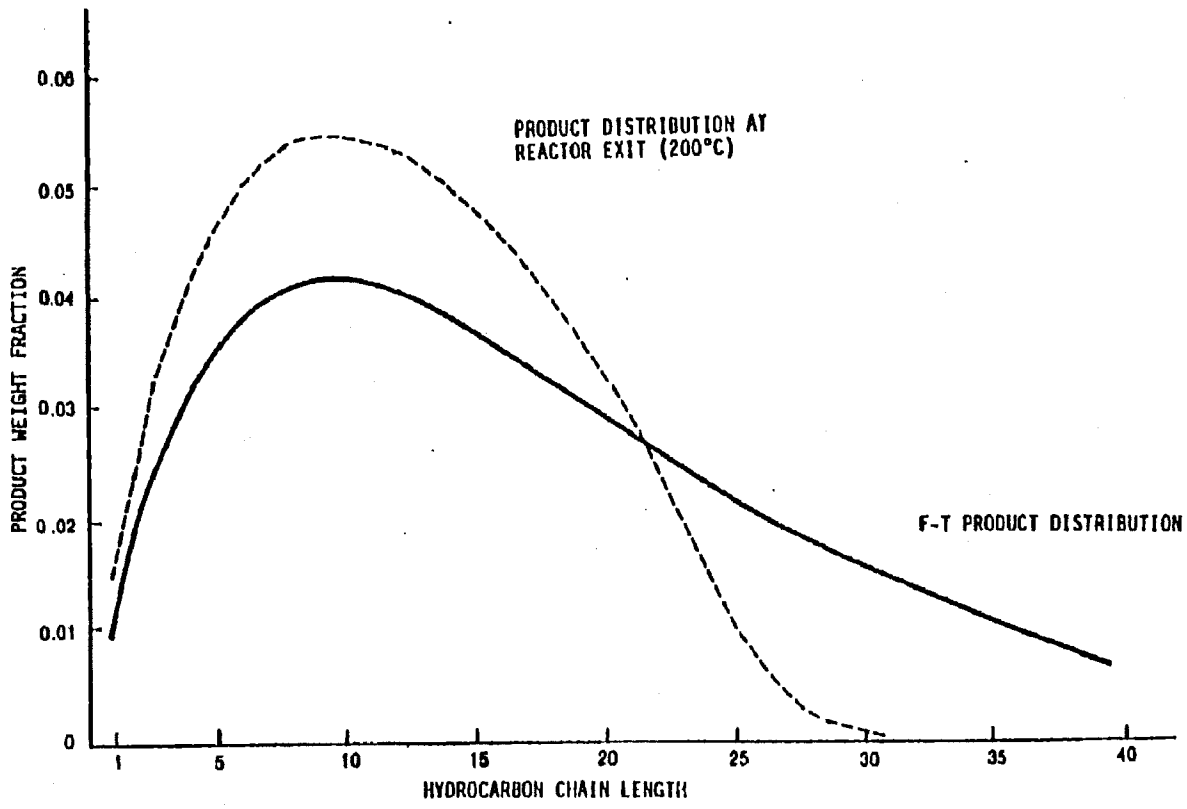

Figure 8-10. Calculated Product Distribution Exiting Reactor, Assuming Vapor-Liquid Equilibrium is Obtained Twice with Intermediate Hydrocaron Vapor Removal. Initial charge is Schulz-Flory with D = 10.

Reference: (75)

approach to a steady-state product distribution, requiring long periods of operation of 150-200 h.

8.3.2 Product Fractionation in the Reactor and Receivers

Heavy hydrocarbon products may come to vapor-liquid equilibrium within the reactor and in the product collection vessels. For example, imagine an experimental system consisting of a reactor operating at 200°C, a wax trap at 80°C, an ambient trap at 25°C, and an oil trap at 0°C. When products of S-F distribution with D = 10 (as in Figure 8-1) are allowed to come to vapor-liquid equilibrium at each successive vessel, the measured product distribution after each vessel is as shown in Figure 8-11.

8.3.3 Recommended Solutions

The effect of product condensation within the reactor and of product fractionation in the reactor and collection system can be minimized in several ways. Synthesis of hydrocarbons for extended periods to produce quantities of product that are large (relative to those that can be retained by the catalyst charge) can produce distributions characteristic of the catalyst rather than of physical phenomena. Similarly, the synthesis and collection of large volumes of product minimizes the effect of condensation of small amounts of material in the collection system.

To determine product distributions from short-term synthesis experiments, thermal desorption of product from the catalyst in an inert gas stream or solvent extraction of product hydrocarbons from the catalyst may allow quantification of the hydrocarbons retained on the catalyst. However, these procedures, especially thermal desorption, may result in hydrocarbon decomposition or coking and thus may alter the product distribution. Solvent extraction of the catalyst, as well as a solvent rinse of the reactor and product collection traps, may yield complete product collection from short runs. However, the problem of loss of high-vapor-pressure components upon reactor pressure release can still be a problem. Long-term operation and collection of large quantities of product,

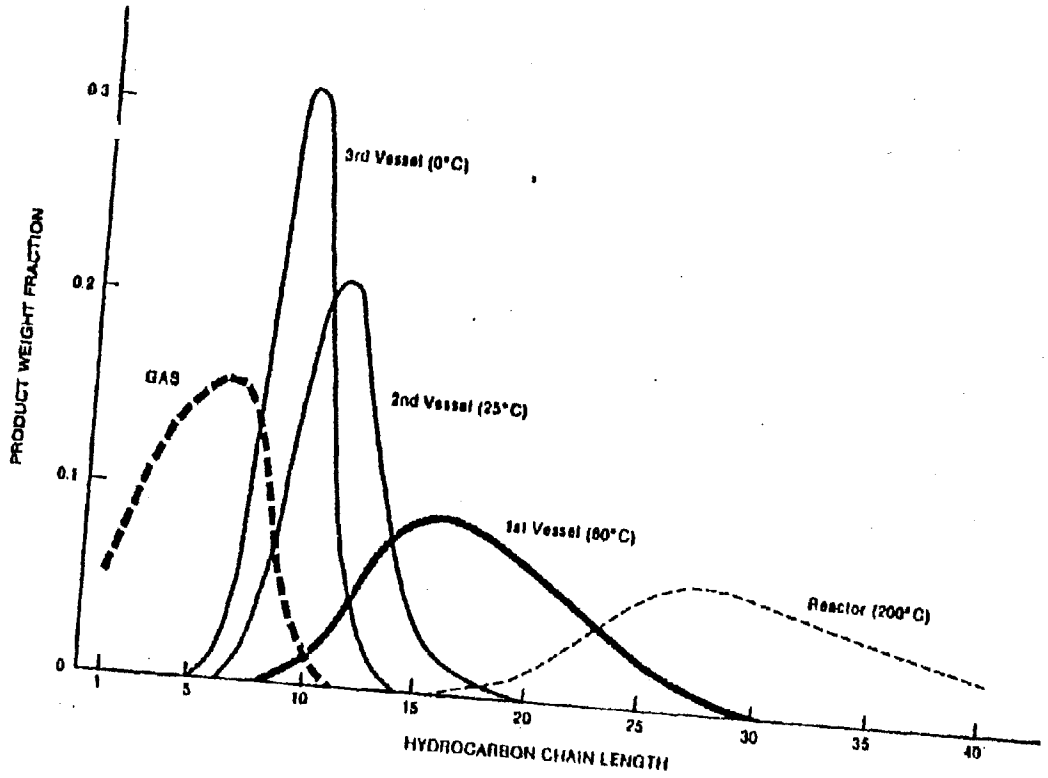

Figure 8-11. Calculated Product Fractions Collected in Successive Vessels, Assuming 50% Conversion of CO + H_2 and Vapor-Liquid Equilibrium Obtained in Each Vessel. Initial hydrocarbon distribution is Schulz-Flory with D = 10.

Reference: (75)

together with a firm assessment of the reactor material balance, should provide the best means of quantifying the intrinsic catalyst product distribution.

8.4 EXPERIMENTAL OBSERVATIONS

8.4.1 Union Carbide

Union Carbide, under a DOE contract (78), has demonstrated some S-F bypass catalysts. Their catalysts have a metal component (MC) and a shape-selective component (SSC). Table 8-3 lists the major catalysts developed for the contract period ending February 1983.

An outstanding catalyst from the standpoint of maximizing motor fuel production is the cobalt-impregnated UCC-101 zeolite catalyst. The product distribution can be compared with that of a conventional F-T iron catalyst that was prepared by UCC and tested in the same reactor (Berty reactor) as all the other catalysts listed in Table 8-3. The Co-UCC-101 shows a comparable gasoline fraction but a much higher fuel oil (diesel) cut. Total motor fuel fraction for this catalyst is 68.9%, compared to 59% for the F-T catalyst.

A hypothetical S-F catalyst in a maximum motor fuel mode could produce almost 72% of the product in the motor fuel range, with the balance distributed as <3% methane and about 9% wax (78). A S-F plot of the product distribution for Sample No. 10011-14-07 is shown in Figure 8-12. UCC claims that the Co-UCC-101 catalyst exceeds the hypothetical S-F catalyst if the carbon consumed in methane formation is redistributed as liquids. This is an interesting contention yet to be experimentally demonstrated.

The Co-UCC-101 catalyst is a 10% cobalt on a UCC-101 carrier. The accounts of testing at 220°C and 250°C are given in Tables 8-4, 8-5, and 8-6. The reactor was a Berty reactor, which is a gas-phase reactor of ultimate gas recycle (Figure 8-13). At 220°C, the conversion was low, in the 7-10% range on CO. At 250°C, the CO conversion increased to the 18-20% range, which is still low,

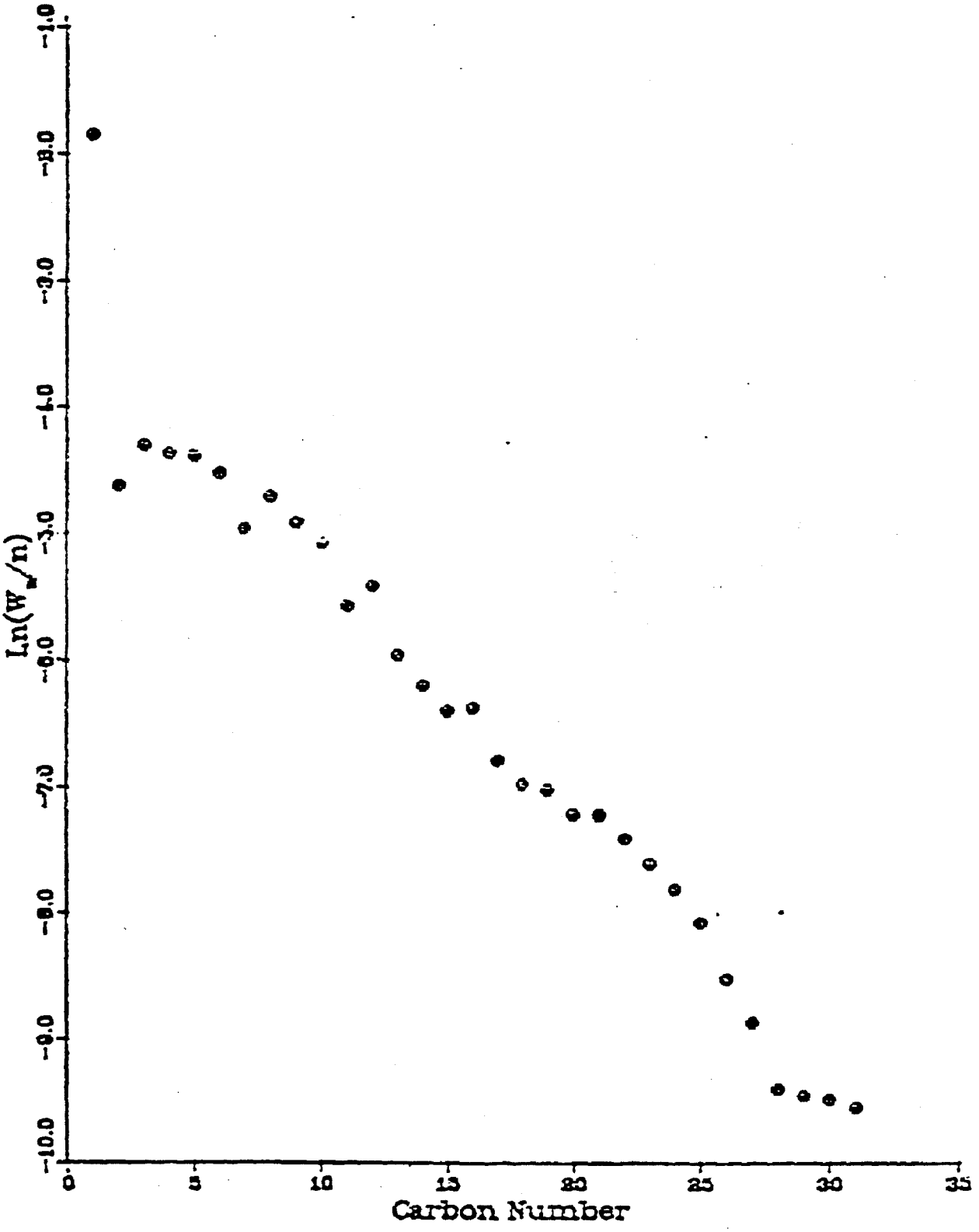

Figure 8-12. Plot of the Hydrocarbon Product Distribution for UCC Sample No. 10011-14-07.

Table 8-3

Union Carbide Catalysts for Synfuel from Syngas

Catalyst	Reference Iron	Fe on UCC-101	Fe/K on UCC-101	Physical Mixtures Fe/K UCC-101	Physical Mixtures Fe/K UCC-104	Pore-Filled Co-UCC-101
C_1-C_2	15	19.4	19.7	16.9	22.8	16.0
C_3-C_4	18	25.5	24.0	23.2	26.7	7.9
Gasoline	42	50.1	42.8	42.3	41.5	44.4
Fuel oil	18	4.9	11.3	14.4	7.8	24.5
Wax	9	0.2	2.3	3.2	1.2	7.2
Oxygenates	<1	<1	<1	<1	<1	<1
Aromatics						
Total motor fuel	59	54.9	54.1	56.7	49.3	68.9

Reference: (78)

Table 8-4

Co-UCC-101 Testing (220°C, Low SV)

RESULT OF SYNGAS OPERATION

RUN NO. 10011-14
CATALYST COBALT-UCC-101 #10042-17 80CC 49.6G (58.1 AFTER RUN,+8.4G)
FEED H2:CO:ARGON OF 50:50: 0 @ 400 CC/MN OR 300 GHSV

RUN & SAMPLE NO.	10011-14-01	011-14-02	011-14-03	011-14-04	011-14-05
FEED H2:CO:AR	50:50: 0	50:50: 0	50:50: 0	50:50: 0	50:50: 0
HRS ON STREAM	6.08	24.58	30.5	55.5	75.33
PRESSURE,PSIG	290	292	291	297	295
TEMP. C	218	219	219	219	219
FEED CC/MIN	400	400	400	400	400
HOURS FEEDING	6.08	18.50	5.92	25.00	19.83
EFFLNT GAS LITER	78.45	398.80	128.50	541.32	435.98
GM AQUEOUS LAYER	12.50	17.58	4.91	23.13	16.27
GM OIL	0.87	2.66	0.99	4.19	3.31
MATERIAL BALANCE					
GM ATOM CARBON %	63.84	102.66	102.35	101.18	102.54
GM ATOM HYDROGEN %	78.70	101.14	101.99	103.85	103.93
GM ATOM OXYGEN %	82.75	109.61	107.59	107.50	107.87
RATIO CHX/(H2O+CO2)	0.2500	0.5099	0.5914	0.5464	0.5853
RATIO X IN CHX	2.3248	2.4265	2.3603	2.3820	2.3974
USAGE H2/CO PRODT	2.0546	2.1192	2.1127	2.1072	2.1066
RATIO CO2/(H2O+CO2)	0.0021	0.0060	0.0054	0.0069	0.0102
K SHIFT IN EFFLNT	0.00	0.00	0.00	0.01	0.01
CONVERSION					
ON CO %	9.96	7.13	7.48	7.61	7.45
ON H2 %	41.27	22.61	21.29	22.04	20.89
ON CO+H2 %	27.25	14.81	14.37	14.92	14.22
PRDT SELECTIVITY,WT %					
CH4	14.43	20.56	17.34	17.78	18.93
C2 HC'S	1.31	1.85	1.59	2.92	2.13
C3H8	1.72	1.64	1.61	1.75	2.01
C3H6=	1.55	3.12	3.11	3.05	2.33
C4H10	2.67	1.97	1.85	1.88	1.83
C4H8=	1.83	3.58	3.76	4.06	3.65
C5H12	3.47	2.19	1.92	2.18	2.09
C5H10=	0.13	0.44	0.44	0.60	0.57
C6H14	5.37	3.18	2.94	2.98	2.73
C6H12= & CYCLO'S	1.01	2.55	3.66	3.17	3.29
C7+ IN GAS	34.47	31.07	30.76	28.68	29.24
LIQ HC'S	32.03	27.86	31.02	30.95	31.19

Reference: (78)

Table 8-4 (Continued)

Co-UCC-101 Testing (200°C, Low SV)

TOTAL	100.00	100.00	100.00	100.00	100.00
SUB-GROUPING					
C1 -C4	23.51	32.72	29.26	31.44	30.89
C5 --420 F	60.64	48.70	48.10	45.84	55.08
420-700 F	13.07	17.08	20.60	19.38	10.92
700-END PT	2.79	1.50	2.05	3.34	3.12
C5+-END PT	76.49	67.28	70.74	68.56	69.11
ISO/NORMAL MOLE RATIO					
C4	0.5628	0.1916	0.1818	0.1180	0.0625
C5	1.0050	0.3383	0.2538	0.1772	0.1242
C6	2.0347	0.8870	0.7712	0.5435	0.4462
C4=	0.0000	0.0000	0.0250	0.0324	0.0404
PARAFFIN/OLEFIN RATIO					
C3	1.0547	0.5000	0.4923	0.5481	0.8262
C4	1.4088	0.5307	0.4756	0.4462	0.4845
C5	25.3125	4.8108	4.2895	3.5094	3.5833
LIQ HC COLLECTION					
PHYS. APPEARANCE	CLEAR OIL	CLEAR OIL	CLEAR OIL	CLEAR OIL	YLW OIL
DENSITY				0.779	0.770
N, REFRACTIVE INDEX				1.4380	1.4364
SIMULT'D DISTILATN					
10 WT % @ DEG F	311	334	344	351	357
16	326	362	381	384	389
50	419	474	513	523	522
84	589	604	645	674	679
90	685	644	674	705	711
RANGE(16-84 %)	263	242	264	290	290
WT % @ 420 F	50.50	33.30	27.00	26.60	25.33
WT % @ 700 F	91.30	94.60	93.40	89.20	87.83

Table 8-5

Co-UCC-101 Testing (250°C, Low SV)

RESULT OF SYNGAS OPERATION

RUN NO. 10011-14
CATALYST CORALT-UCC-101 #10042-17 80CC 49.6G (58.1G AFTER RUN,+8.4G)
FEED H2:CO:ARGON OF 50:50: 0 @ 400 CC/MN OR 300 GHSV

RUN & SAMPLE NO.	10011-14-06	011-14-07	011-14-08	011-14-09	011-14-10
FEED H2:CO:AR	50:50: 0	50:50: 0	50:50: 0	50:50: 0	50:50: 0
HRS ON STREAM	78.41	95.41	102.33	119.5	126.25
PRESSURE,PSIG	289	291	290	292	296
TEMP. C	251	251	251	252	252
FEED CC/MIN	400	400	400	400	400
HOURS FEEDING	3.08	20.08	6.92	24.09	6.75
EFFLNT GAS LITER	52.81	314.78	109.15	384.59	109.82
GM AQUEOUS LAYER	7.39	48.15	16.92	58.91	16.63
GM OIL	2.32	15.10	5.75	20.00	6.97
MATERIAL BALANCE					
GM ATOM CARBON %	110.28	101.91	102.50	103.96	107.53
GM ATOM HYDROGEN %	110.43	102.79	105.44	106.50	109.35
GM ATOM OXYGEN %	116.15	108.31	108.40	109.30	111.44
RATIO CHX/(H2O+CO2)	0.8178	0.7923	0.8112	0.8290	0.8758
RATIO X IN CHX	2.3970	2.3427	2.3289	2.3247	2.3130
USAGE H2/CO PRODT	1.9268	2.0001	2.0096	2.0198	2.0200
RATIO CO2/(H2O+CO2)	0.0782	0.0452	0.0414	0.0386	0.0392
K SHIFT IN EFFLNT	0.05	0.03	0.03	0.02	0.02
CONVERSION					
ON CO %	26.16	25.34	26.02	26.05	26.81
ON H2 %	55.47	56.48	56.46	56.43	56.87
ON CO+H2 %	40.83	40.98	41.45	41.43	41.96
PRDT SELECTIVITY,WT %					
CH4	17.85	15.81	15.26	15.11	14.54
C2 HC'S	2.51	1.98	1.87	1.83	1.83
C3H8	2.54	1.90	1.85	1.79	1.74
C3H6=	2.03	2.18	2.13	2.15	2.04
C4H10	2.15	1.63	1.55	1.50	1.49
C4H8=	3.45	3.46	3.34	3.38	3.31
C5H12	3.08	2.38	2.24	2.10	1.96
C5H10=	3.89	3.86	3.76	3.80	0.47
C6H14	3.80	3.24	2.74	2.81	2.70
C6H12= & CYCLO'S	2.94	3.31	3.20	4.65	2.72
C7+ IN GAS	15.62	16.88	15.87	15.62	14.37
LIQ HC'S	40.15	43.37	46.19	45.26	52.84

Reference: (78)

Table 8-5 (Continued)

Co-UCC-101 Testing (250°C, Low SV)

TOTAL	100.00	100.00	100.00	100.00	100.00
SUB-GROUPING					
C1 -C4	30.52	26.94	26.01	25.76	24.94
C5 -420 F	51.42	47.51	53.21	46.77	51.29
420-700 F	14.05	21.25	16.17	22.67	18.49
700- END PT	4.01	4.29	4.62	4.80	5.28
C5+-END PT	69.48	73.06	73.99	74.24	75.06
ISO/NORMAL MOLE RATIO					
C4	0.1779	0.1718	0.1617	0.1431	0.1338
C5	0.4215	0.3520	0.3112	0.2866	0.2531
C6	0.8722	0.7599	0.5689	0.6935	0.6801
C4=	0.0377	0.0399	0.0420	0.0449	0.0434
PARAFFIN/OLEFIN RATIO					
C3	1.1944	0.8323	0.8293	0.7937	0.8122
C4	0.6007	0.4538	0.4489	0.4293	0.4358
C5	0.7708	0.5999	0.5787	0.5362	0.0253
LIQ HC COLLECTION					
PHYS. APPEARANCE	---	CLEAR OIL	---	CLEAR OIL	---
DENSITY	---	0.764	---	0.768	---
N, REFRACTIVE INDEX	---	1.4330	---	1.4335	---
SIMULT'D DISTILATN					
10 WT % @ DEG F	---	293	---	301	---
16	---	327	---	332	---
50	---	463	---	473	---
84	---	656	---	665	---
90	---	699	---	705	---
RANGE(16-84 %)	---	329	---	333	---
WT % @ 420 F	---	41.10	---	39.30	---
WT % @ 700 F	---	90.10	---	89.40	---

Table 8-6

Co-UCC-101 Testing (250°C, High SV)

RESULT OF SYNGAS OPERATION

RUN NO. 10011-14
CATALYST COBALT-UCC-101 #10042-17 80CC 49.6G (58.1G AFTER RUN,-8.4G)
FEED H2:CO:ARGON OF 50:50: 0 @ 400 CC/MN OR 300 GHSV

RUN & SAMPLE NO.	10011-14-11	011-14-12	011-14-13	011-14-14	011-14-15
FEED H2:CO:AR	50:50: 0	50:50: 0	50:50: 0	50:50: 0	50:50: 0
HRS ON STREAM	143.67	150.25	168.83	174.16	192.99
PRESSURE,PSIG	290	298	300	292	292
TEMP. C	252	252	252	252	252
FEED CC/MIN	400	800	800	800	800
HOURS FEEDING	24.17	6.58	18.58	5.33	18.83
EFFLNT GAS LITER	388.93	231.21	638.74	183.69	652.57
GM AQUEOUS LAYER	59.55	19.72	58.12	16.32	58.69
GM OIL	24.94	8.23	22.22	6.80	73.00
MATERIAL BALANCE					
GM ATOM CARBON %	107.63	97.34	93.62	95.12	94.87
GM ATOM HYDROGEN %	107.79	103.91	100.53	101.92	101.82
GM ATOM OXYGEN %	111.36	97.72	97.17	96.80	97.67
RATIO CHX/(H2O+CO2)	0.8813	0.9813	0.8292	0.9180	0.8655
RATIO X IN CHX	2.3038	2.3413	2.3820	2.3605	2.3765
USAGE H2/CO PRODT	2.0271	2.0921	2.0958	2.0943	2.0908
RATIO CO2/(H2O+CO2)	0.0358	0.0246	0.0228	0.0243	0.0253
K SHIFT IN EFFLNT	0.02	0.02	0.02	0.02	0.02
CONVERSION					
ON CO %	26.73	20.79	18.91	20.24	19.52
ON H2 %	57.60	41.13	40.61	41.29	40.90
ON CO+H2 %	42.17	31.30	30.15	31.13	30.59
PROT SELECTIVITY,WT %					
CH4	14.28	16.07	18.07	17.04	17.78
C2 HC'S	1.72	1.84	2.09	1.92	2.02
C3H8	1.56	1.86	1.90	1.85	1.92
C3H6=	1.96	2.11	2.21	2.15	2.12
C4H10	1.33	1.52	1.57	1.50	1.58
C4H8=	3.09	3.27	3.43	3.32	3.56
C5H12	1.81	1.92	1.96	1.93	2.00
C5H10=	3.30	3.70	0.59	3.47	2.13
C6H14	2.43	2.36	2.50	2.50	2.65
C6H12= & CYCLO'S	3.06	3.28	1.41	1.43	1.46
C7+ IN GAS	12.72	17.45	15.49	15.03	15.06
LIQ HC'S	52.74	44.63	48.77	47.86	47.72

Reference: (78)

Table 8-6 (Continued)

Co-UCC-101 Testing (250°C, High SV)

TOTAL	100.00	100.00	100.00	100.00	100.00
SUB-GROUPING					
C1 -C4	23.94	26.67	29.28	27.79	28.98
C5 -420 F	44.42	44.10	40.19	41.83	42.01
420--700 F	24.47	21.51	22.24	22.59	21.28
700--END PT	7.17	7.72	8.29	7.80	7.73
C5+-END PT	76.06	73.33	70.72	72.21	71.02
ISO/NORMAL MOLE RATIO					
C4	0.1269	0.0913	0.0845	0.0978	0.0788
C5	0.2401	0.1693	0.1384	0.1425	0.1537
C6	0.6401	0.5284	0.4139	0.4184	0.4853
C4=	0.0459	0.0399	0.0438	0.0442	0.0493
PARAFFIN/OLEFIN RATIO					
C3	0.7614	0.8438	0.8203	0.8223	0.8629
C4	0.4168	0.4481	0.4427	0.4352	0.4291
C5	0.5331	0.5063	3.2230	0.5411	0.9145
LIQ HC COLLECTION					
PHYS. APPEARANCE	CLDY OIL	CLDY OIL	CLDY OIL	CLDY OIL	CLDY OIL
DENSITY	0.767	0.774	0.771	0.771	0.769
N, REFRACTIVE INDEX	1.4332	1.4362	1.4348	1.4342	1.4337
SIMULT'D DISTILAIN					
10 WT % @ DEG F	299	323	314	320	311
16	330	344	336	341	335
50	471	505	490	485	476
84	680	713	710	702	702
90	730	767	757	756	756
RANGE(16-84 %)	350	369	374	361	367
WT % @ 420 F	40.00	34.50	37.40	36.50	39.20
WT % @ 700 F	86.40	82.70	83.00	83.70	83.80

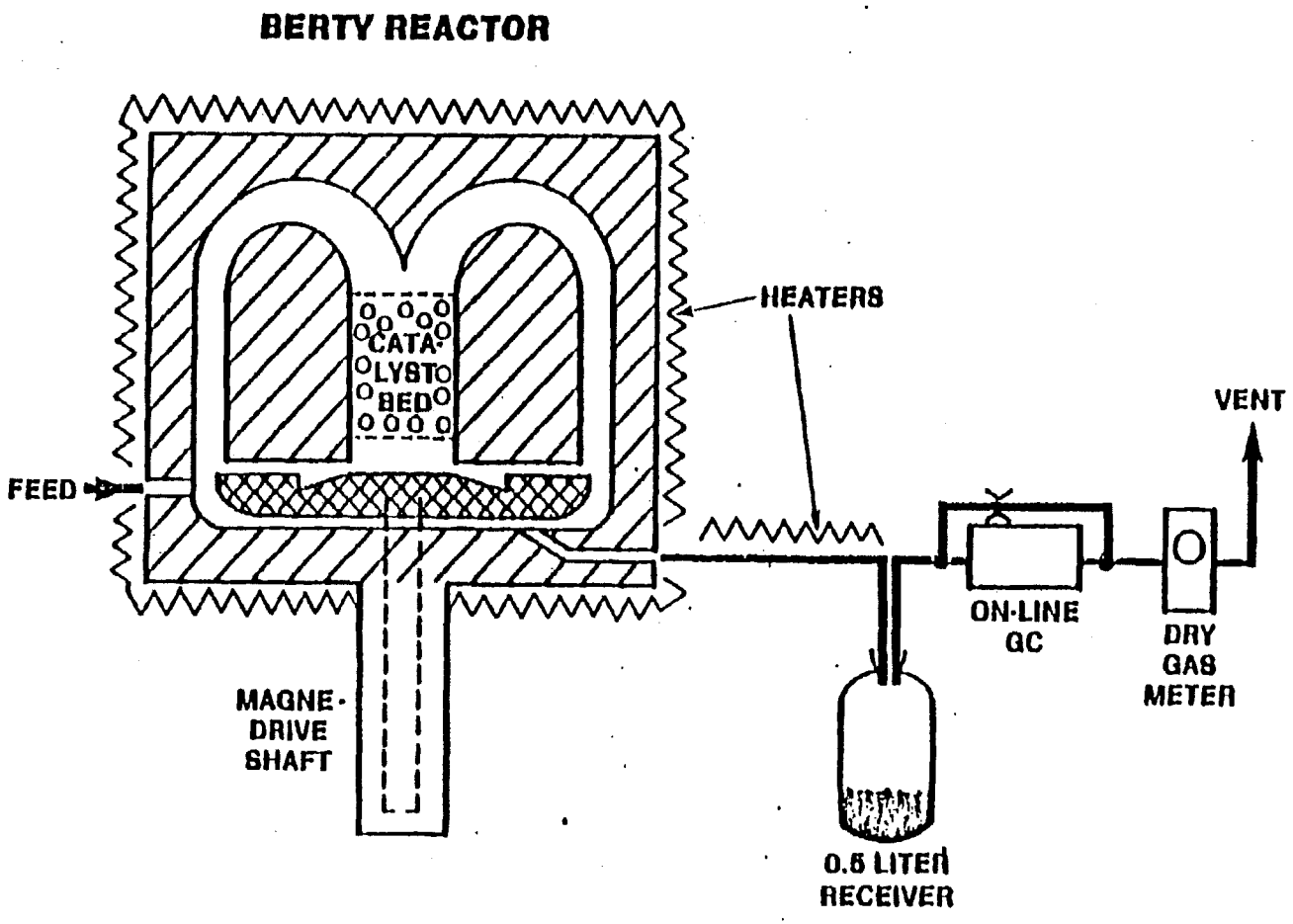

Figure 8-13. Berty Reactor

Reference: (79)

although UCC claimed this to be reasonable. The H_2/CO usage (USAGE H_2/CO PROD) was high, meaning that the catalyst lacked the CO shift capability.

In summary, the Co-UCC-101 catalyst shows some sign of S-F bypass, but as a synthesis catalyst for slurry-phase application, it must acquire a higher CO shift activity and a higher CO conversion capability.

For gasoline production, Fe on UCC-101 shows a maximum of 50.1% of total product (Table 8-3). This catalyst produced only small amounts of diesel and practically no wax. Unfortunately, no test data are given in the reference.

As a next phase of the DOE contract, Union Carbide is to optimize the peformance of these experimental catalysts. The judgment of whether or by how much the S-F distribution can be exceeded showed await the outcome of this phase. Comprehensive documentation of the overall work would be valuable because it will be reviewed by many who are unfamiliar with the preceding progress reports.

8.4.2 Air Products and Chemicals

Under DOE Contract De-AC22-80PC30021, Air Products has a 3-year research program, started in October 1980, to develop catalysts for synfuels from syngas in slurry phase (80).

Air Products is aware of experimental artifacts that lead to an impression of S-F bypass. These are:

- Reactor temperature gradient
- Insufficient time to reach steady state
- Volatilization and condensation differences among products

They sought to exclude these factors from the interpretation of test results.

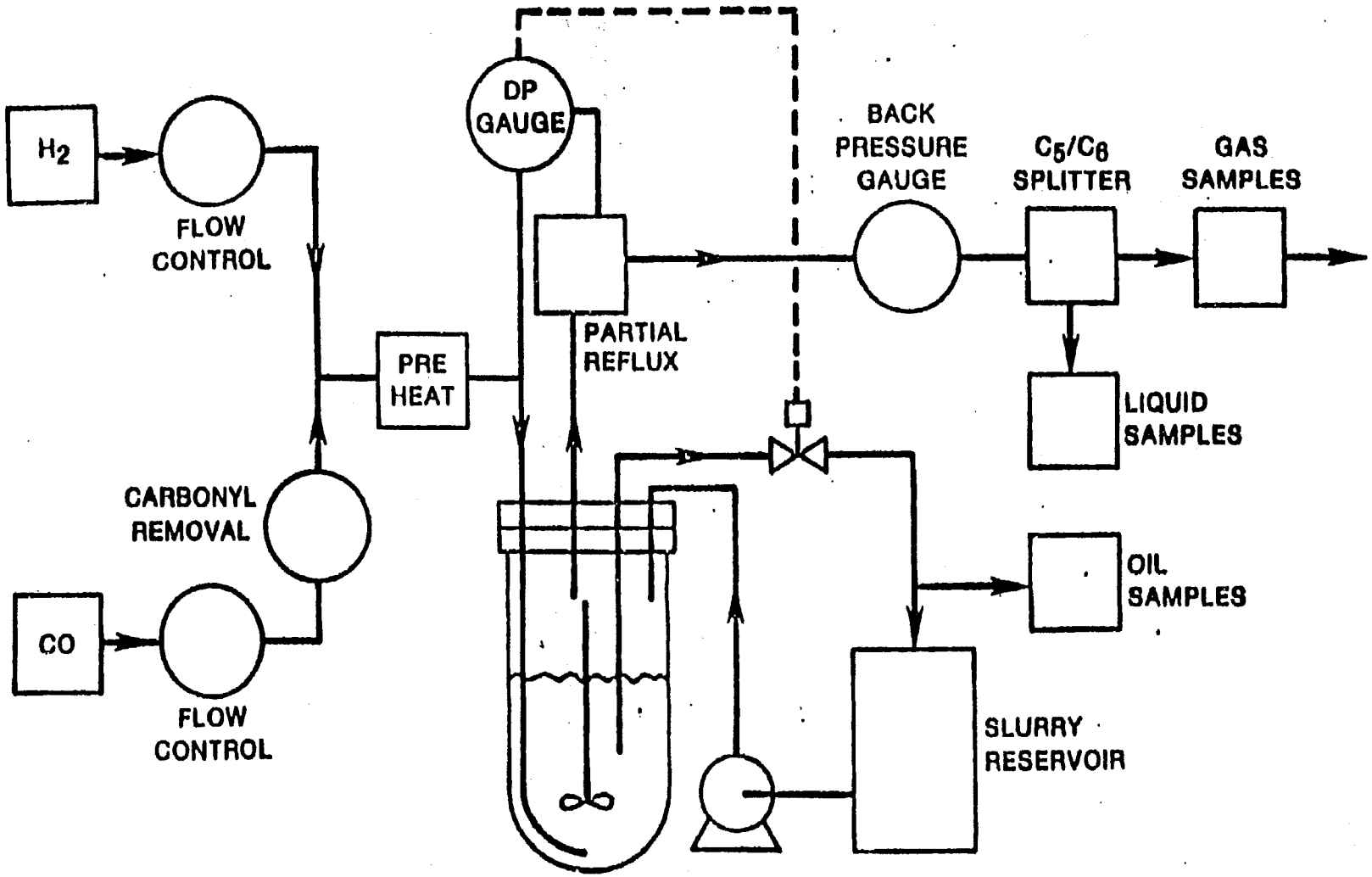

Figure 8-14. Continuous, Automated Fischer-Tropsch Slurry Reactor

Reference: (74)

Four catalysts were tested in a slurry-phase reactor (Figure 8-14). The results are given in Table 8-7. The product selectivities are given for C_1, C_5-C_{11} (gasoline), C_9-C_{25} (diesel), and C_{26}+ (wax). The catalysts included a SASOL-type iron catalyst as the baseline and three experimental catalysts identified as A1, A2, and B. (No details of these catalysts are available.) Product distributions for these catalysts, by carbon number and by hydrocarbon types, are given in Figures 8-15 through 8-19. The S-F bypass capability of the experimental catalysts is seen to a certain extent. As an example, Figure 8-20 shows the S-F plots for catalyst A2 and for the baseline catalyst. An apparent abnormality is evident with Curve a, which is for A2 operating at 237°C, CO/H_2 = 1.0, and a pressure of 2.21 MPa. (The use of "M" is confusing. It is not clear here whether M = 10^3 or M = 10^6. If the latter, p = 320 psia.) Air Products points out that Catalyst B, operating with CO/H_2 = 2.0 (Figure 8-19), shows a diesel selectivity of 67.3 wt%. This is beyond what is predicted by a hypothetical S-F model operating at a maximum diesel model. Such a model predicts a diesel selectivity of 54.1%; therefore, Catalyst B in Figure 8-19 exceeded the S-F distribution by 24%.

Interestingly, the baseline iron catalyt showed a deviation from the S-F-type distribution when the CO/H_2 mole ratio was increased beyond 1.4 (Table 8-7). The trend is illustrated in Figure 8-21. Curve C is for CO/H_2 = 0.5 and shows a typical S-F pattern. Curve B is for CO/H_2 = 1.4 and still obeys the S-F distribution, although minor abnormalities start to appear. Curve A is for CO/H_2 = 2.8, which simulates perhaps the most CO-rich syngas obtainable from advanced gasifiers such as the Shell-Koppers gasifier (Chapter 5). Here, the plot roughly consists of two segments at a carbon number of ten. It is speculated that the segmentation of the S-F plot is the result of reincorporation of olefinic primary products (83). This is plausible because an increase in CO/H_2 ratio has been shown to increase light olefin production (74). Furthermore, olefin reincorporation could be magnified in a well-stirred reactor such as the one used by Air Products.

The demonstration by Air Products that their experimental catalysts show higher selectivites toward motor fuels than the S-F distribution is encouraging. Whether this is a result of product reincorporation that obeys the nonselective

Table 8-7

Summary of Selected Slurry-Phase Fischer-Tropsch Results

Catalyst	P MPa	T °C	GHSV h^{-1}	CO/H_2	Activity mol syngas/kg/h	Selectivity wt%			
						C_1	C_5-C_{11}	C_9-C_{25}	C_{26}+
Fe_2O_3 (baseline)	3.31	280	250	0.5	26.2	17.4	37.6	17.3	0.1
	3.17	248	146	1.4	10.2	7.4	39.9	30.3	1.7
	3.14	277	145	1.4	20.8	6.8	41.1	36.2	2.7
	3.10	281	183	2.8	14.3	4.7	23.8	39.9	12.7
A1	2.03	252	318	0.9	9.9	9.6	41.3	50.8	0.1
A2	2.21	237	307	1.0	13.9	6.2	9.8	46.1	26.8*
	1.12	241	297	1.0	11.1	4.3	23.7	44.5	23.4
B	2.07	247	325	1.0	44.9	10.7	38.8	44.7	7.8
	2.08	250	348	2.0	30.6	6.5	28.9	67.3	5.4

*64.0% C_{18}-C_{35}

Reference: (74)

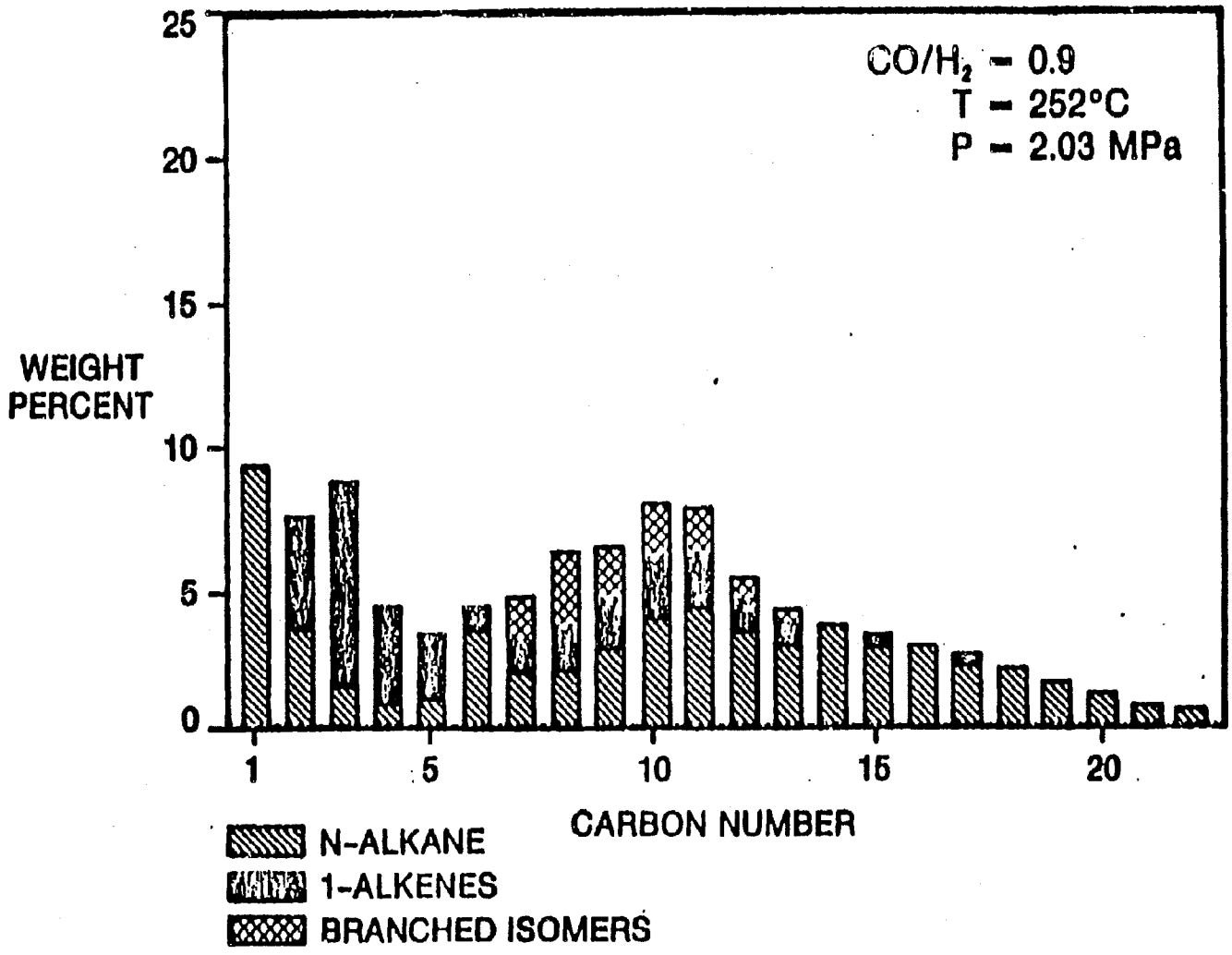

Figure 8-15. Hydrocarbon Weight Distribution for Catalyst A1

Reference: (74)

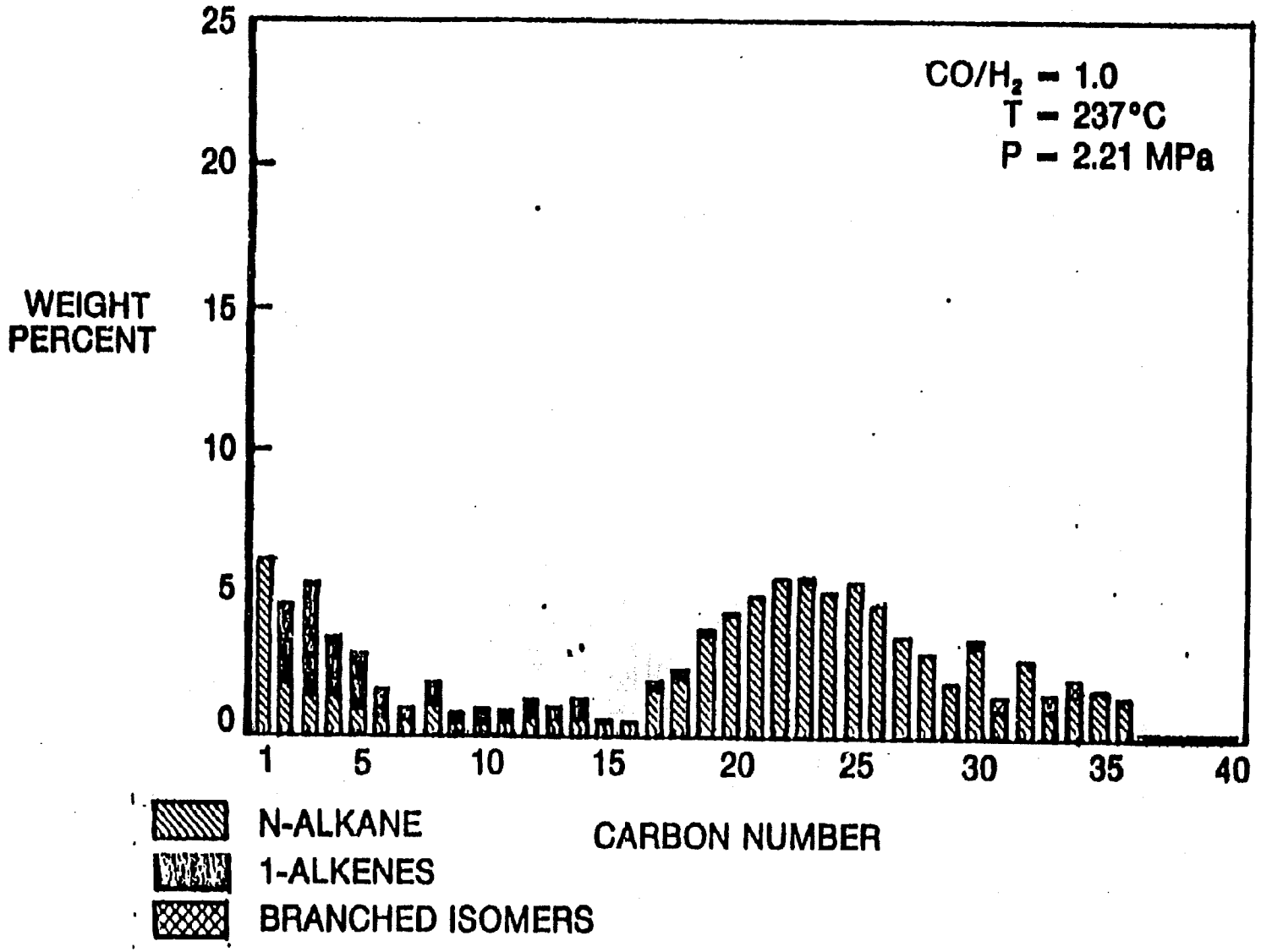

Figure 8-16. Hydrocarbon Weight Distribution for Catalyst A2 (at 237°C, 2.21 MPa)

Reference: (74)

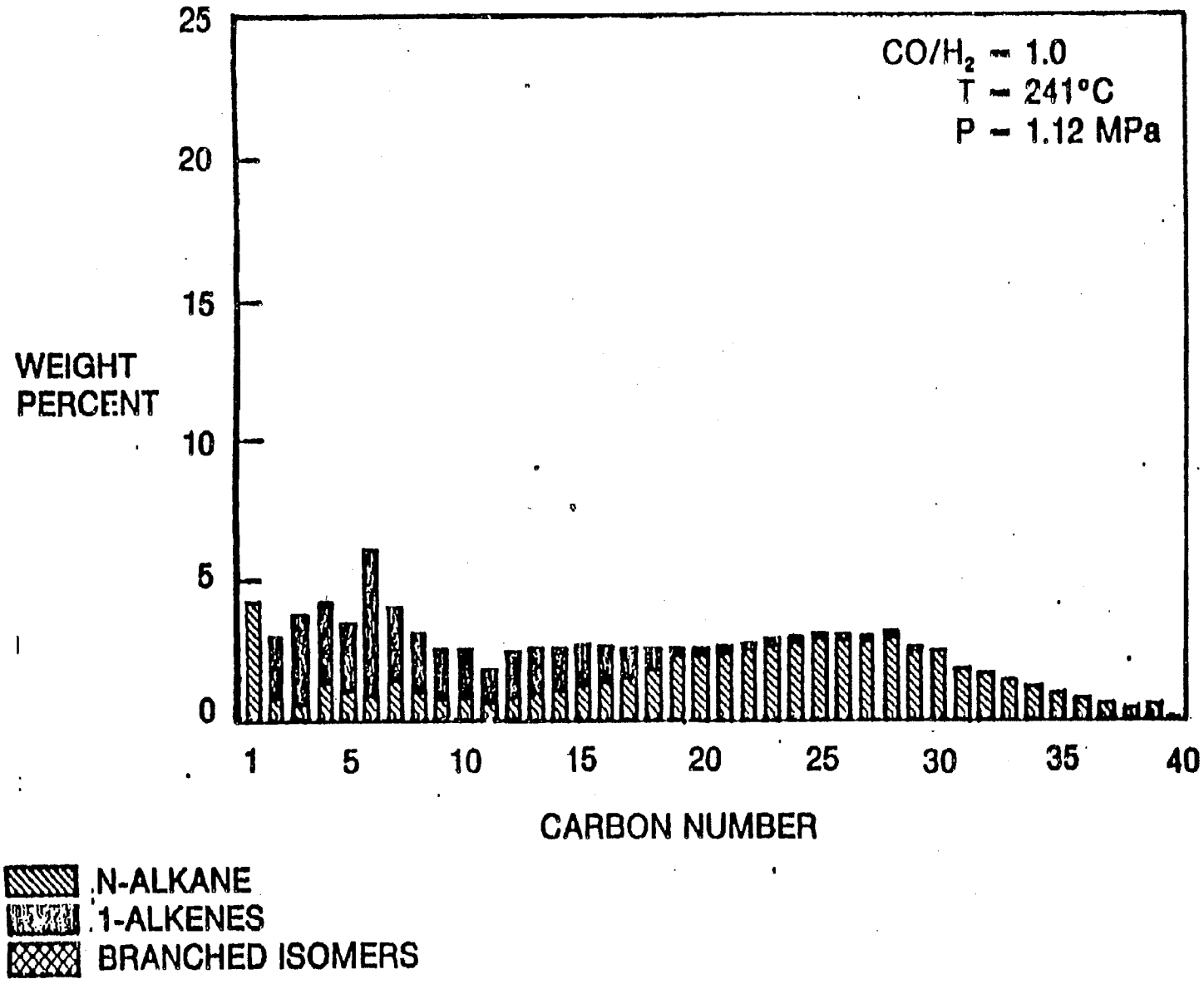

Figure 8-17. Hydrocarbon Weight Distribution for Catalyst A2 (at 241°C, 1.12 MPa)

Reference: (74)

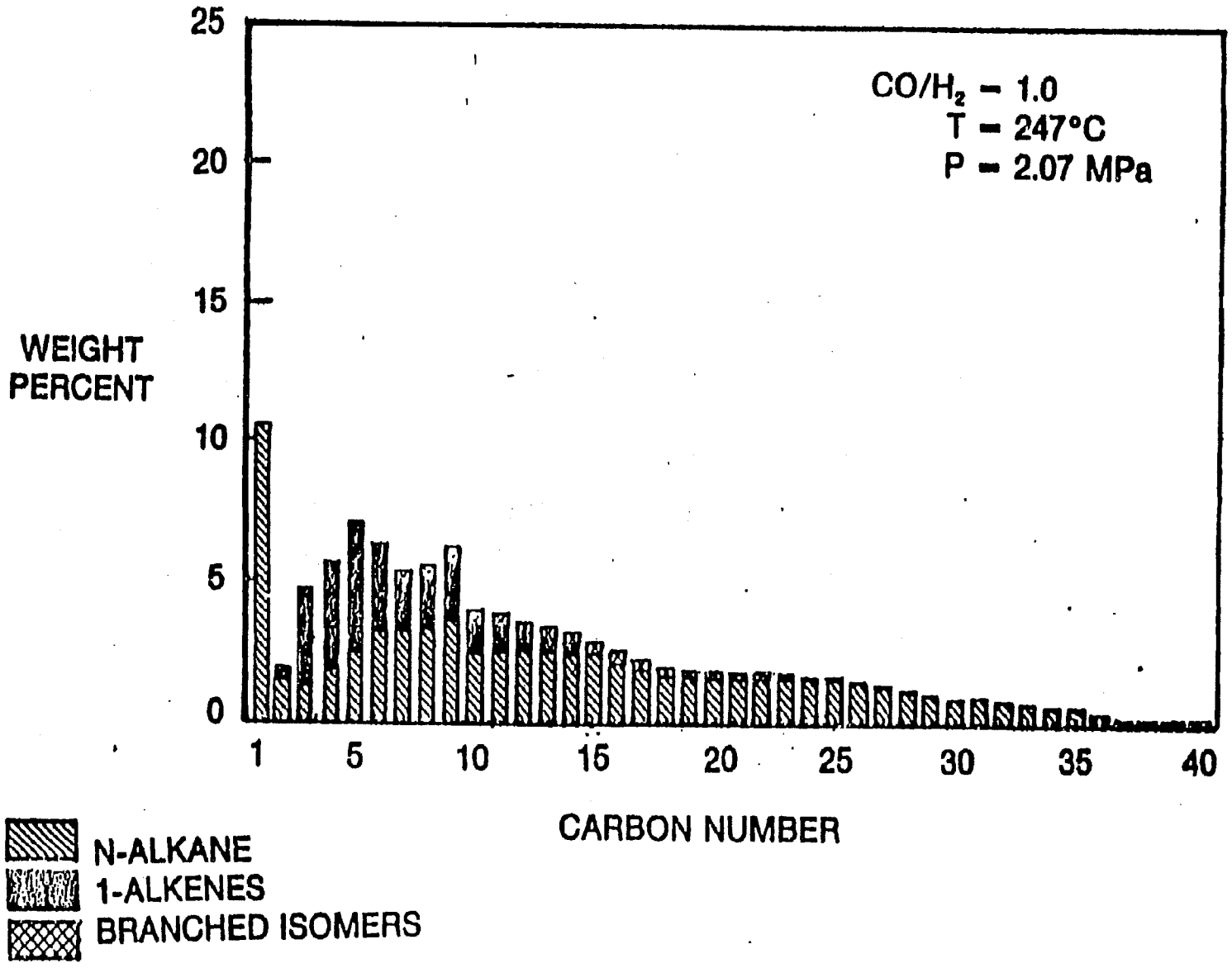

Figure 8-18. Hydrocarbon Weight Distribution for Catalyst B (at 247°C, 2.07 MPa)

Reference: (74)

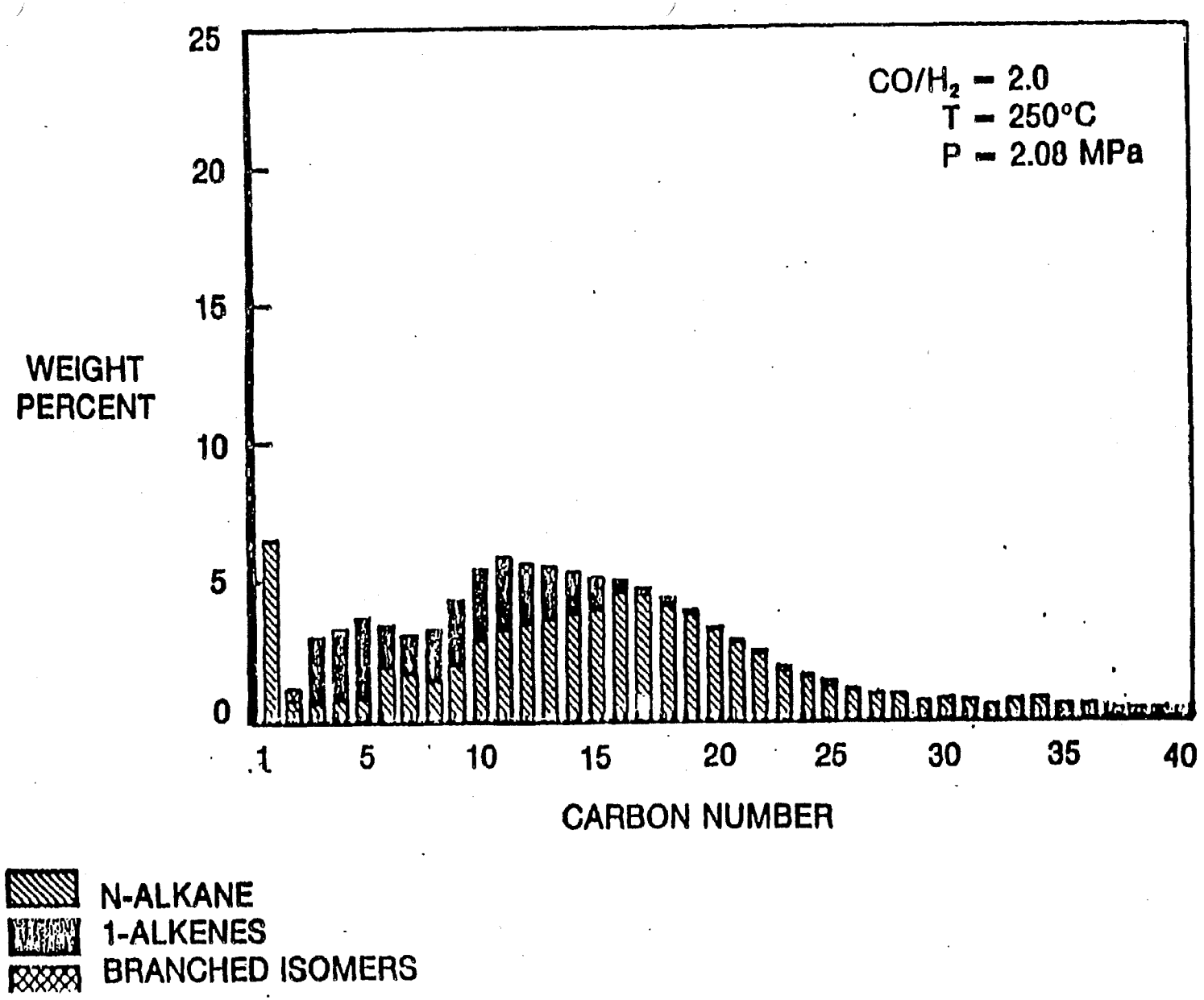

Figure 8-19. Hydrocarbon Weight Distribution for Catalyst B (at 250°C, 2.08 MPa)

Reference: (74)

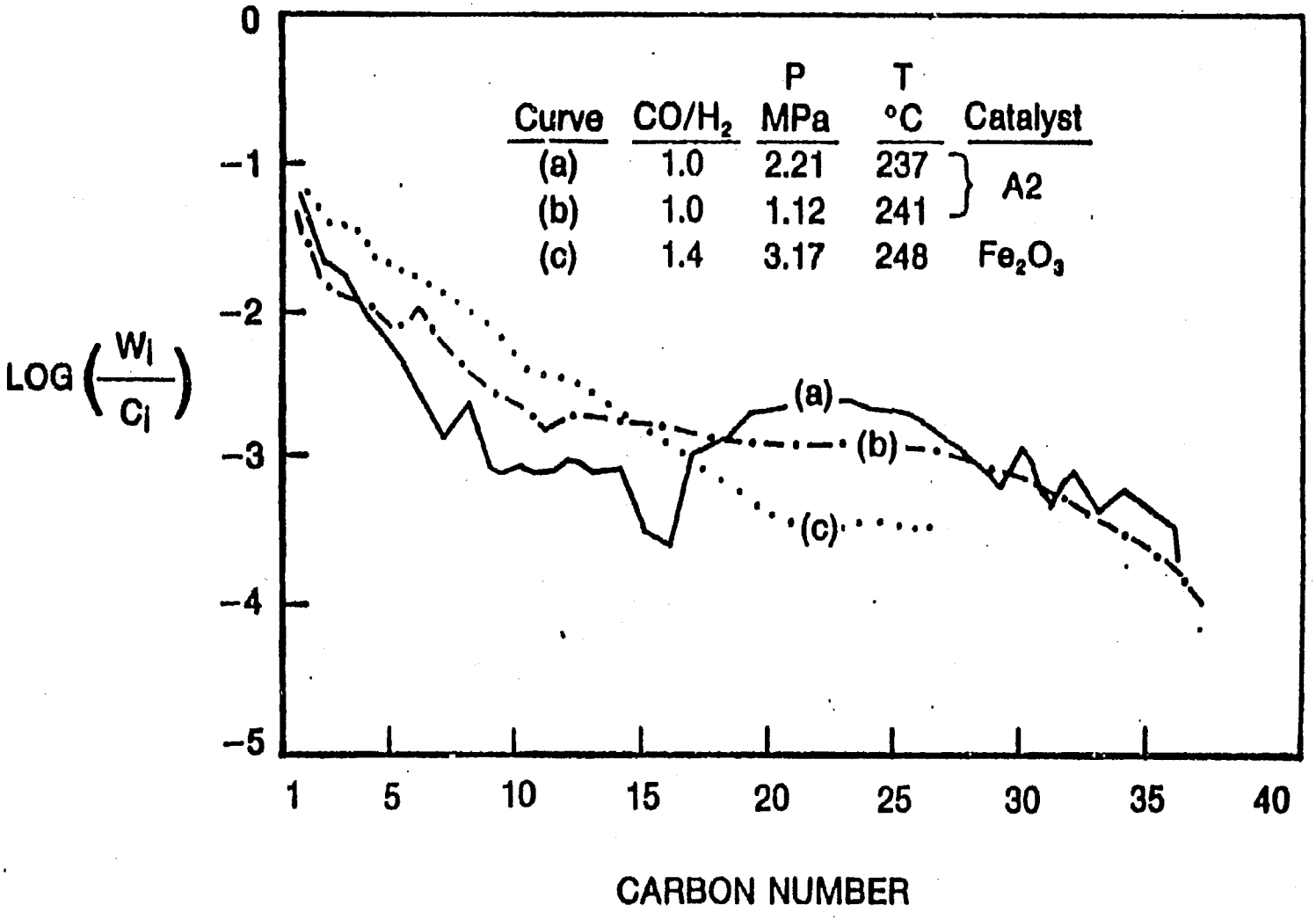

Figure 8-20. Hydrocarbon Schulz-Flory Distribution for Slurry Catalyst A2

Reference: (74)

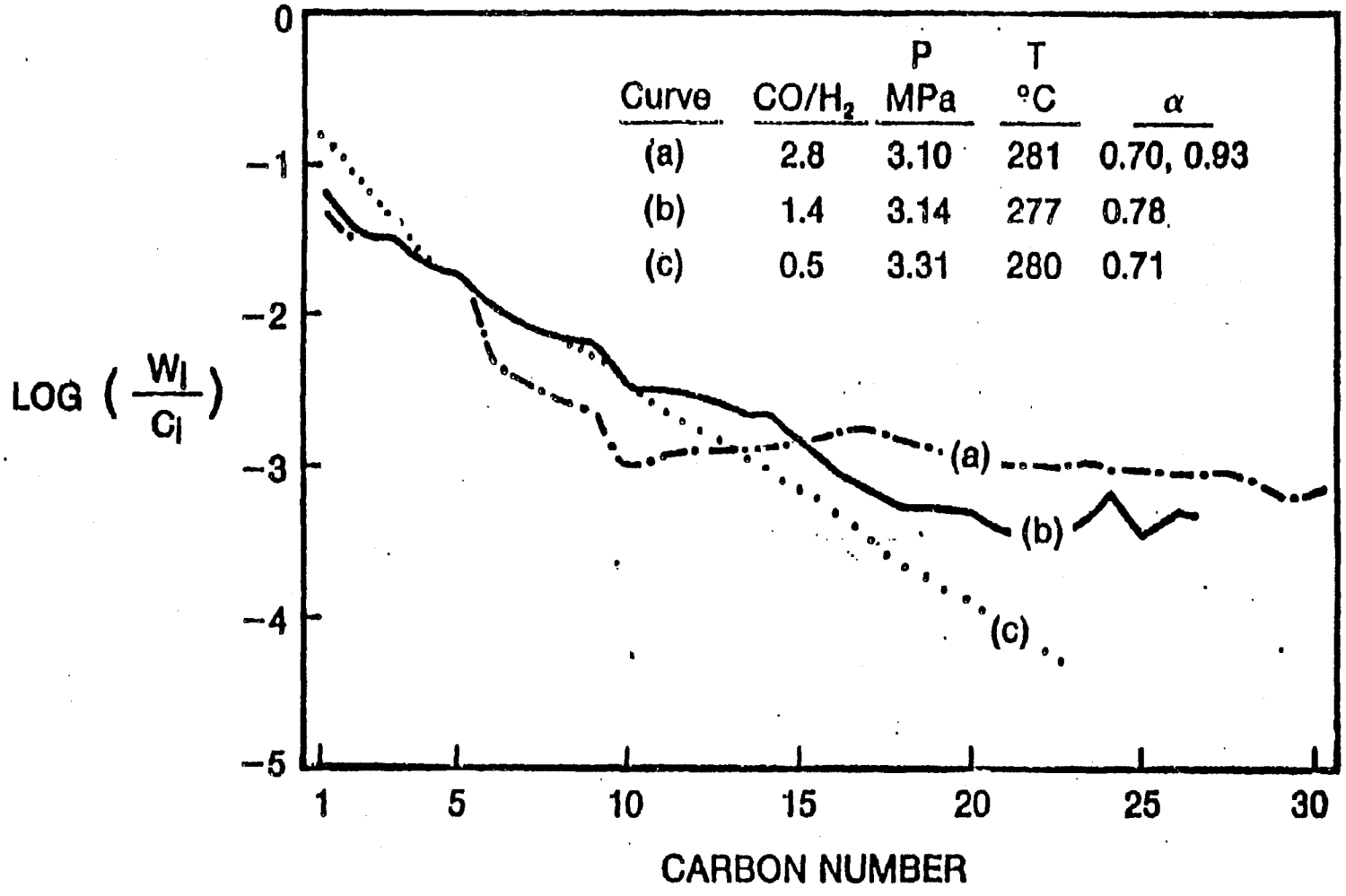

Figure 8-21. Hydrocarbon Schulz-Flory Distribution for Fe_2O_3

Reference: (74)

polymerization mechanism deserves further investigation. Another noteworthy discovery by Air Products is the effect of CO/H_2 on olefin formation. All this work was conducted in a 20-50% conversion range (80), and more work at higher conversion is needed.

8.4.3 Olefin Incorporation

Olefins are primary products of slurry-phase F-T reactions (84). The work by Air Products not only supports this but also provides evidence that the olefin selectivity increases with an increase in CO/H_2 ratio (74). The Air Products data are shown as Figures 8-22, 8-23 and 8-24, which correspond to CO/H_2 values of 0.5, 1.4, and 2.8, respectively. Note that the "1-ALKANE" fraction increases with an increase in CO/H_2 value.

Since olefins constitute a major fraction of primary F-T products, their reincorporation in secondary reactions would substantially alter product distribution. A catalyst that enhances this secondary reaction could yield, for example, much more motor fuels than the S-F distribution allows. Indeed, Air Products speculates that this is the main reason for the S-F bypass by their experimental catalysts (74). An experimental investigation of olefin incorporation was conducted by Dwyer (85). In one test, he introduced 2.7 mol% ethylene in a syngas of H_2/CO mole ratio of 3 and followed the fate of ethylene as it was reacted over iron crystal at 6 atm and 300°C. The results are shown in Figure 8-25. As can be seen in this plot, the predominant reation was hydrogenation to ethane, but some ethylene was incorporated as C_4 and C_5 products. This is shown in Figure 8-26.

To further demonstrate the olefin incorporation, another test was made where ethylene concentration was varied while holding other conditions constant, namely, 300°C, 6 atm, and $H_2/CO = 3.0$. After 90 min. residence time, the product distributions were as shown in Figure 8-27. The ethylene mole percent ranged from 0 to 3.5% (partial pressure of 160 torr). The figure offers evidence that ethylene is indeed incorporated. A rather striking finding is that methane yield is drastically reduced by the presence of ethylene. Another noteworthy effect is

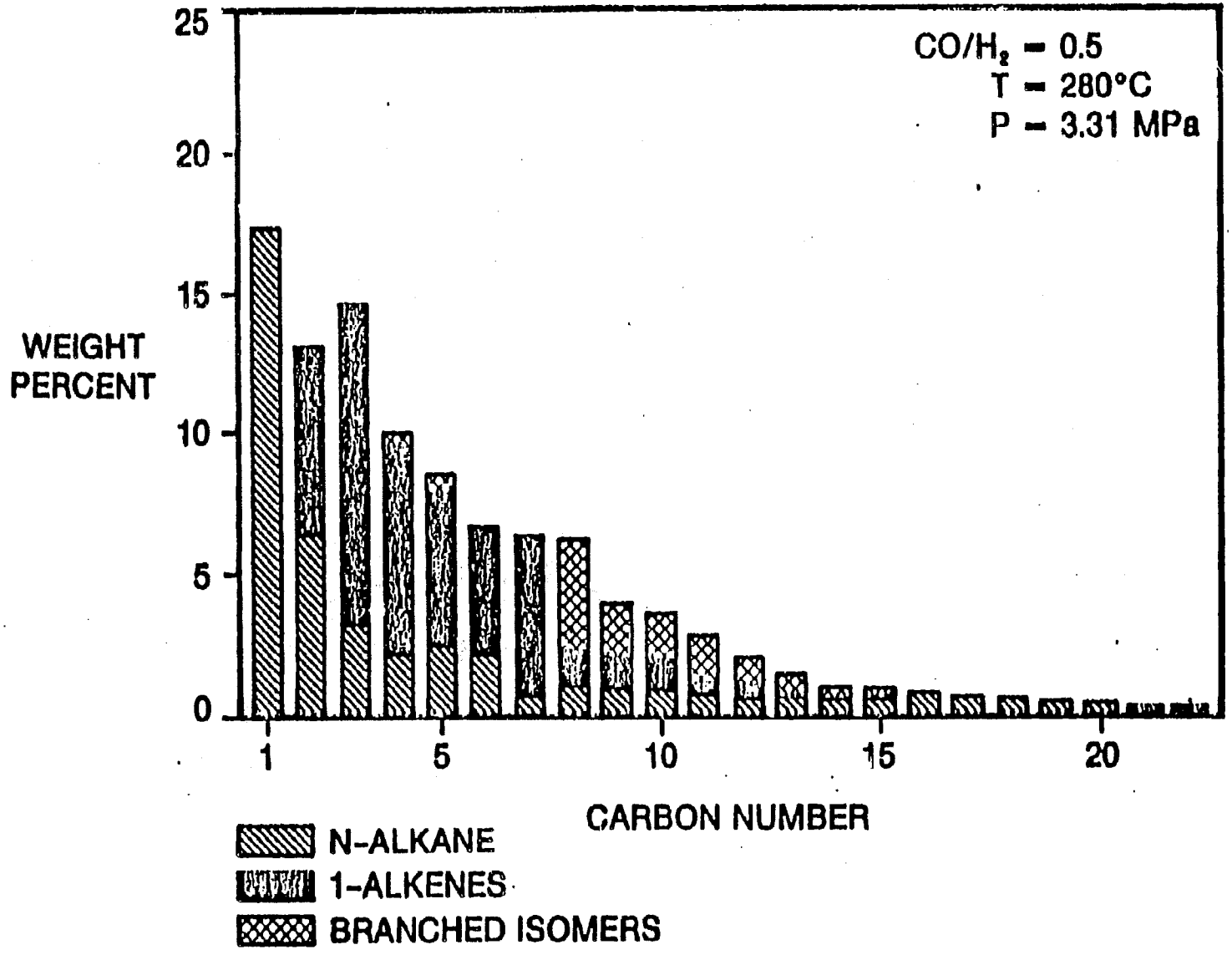

Figure 8-22. Hydrocarbon Weight Distribution for Fe_2O_3 (at 280°C, 3.31 MPa)

Reference: (74)

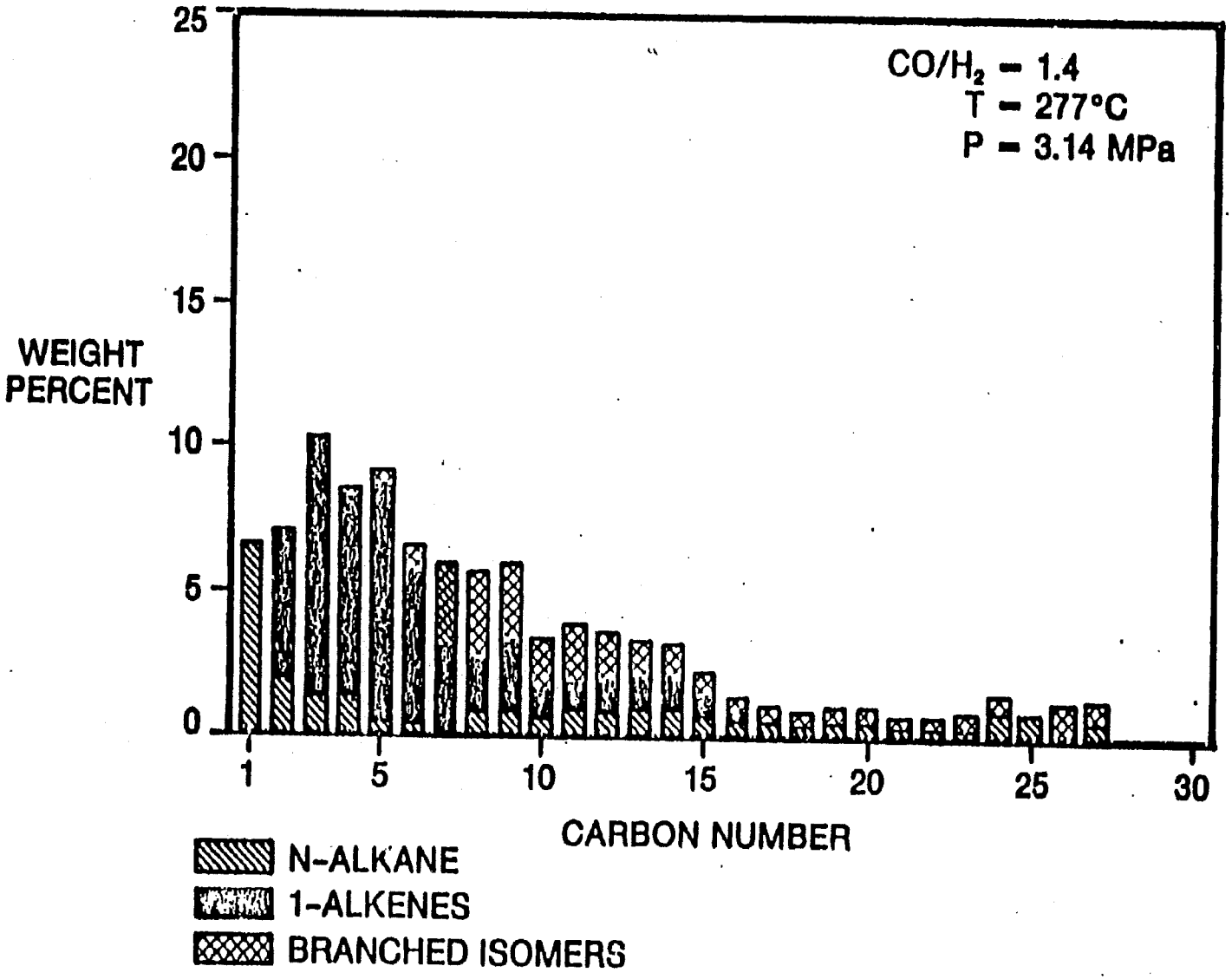

Figure 8-23. Hydrocarbon Weight Distribution for Fe_2O_3 (at 277°C, 3.14 MPa)

Reference: (74)

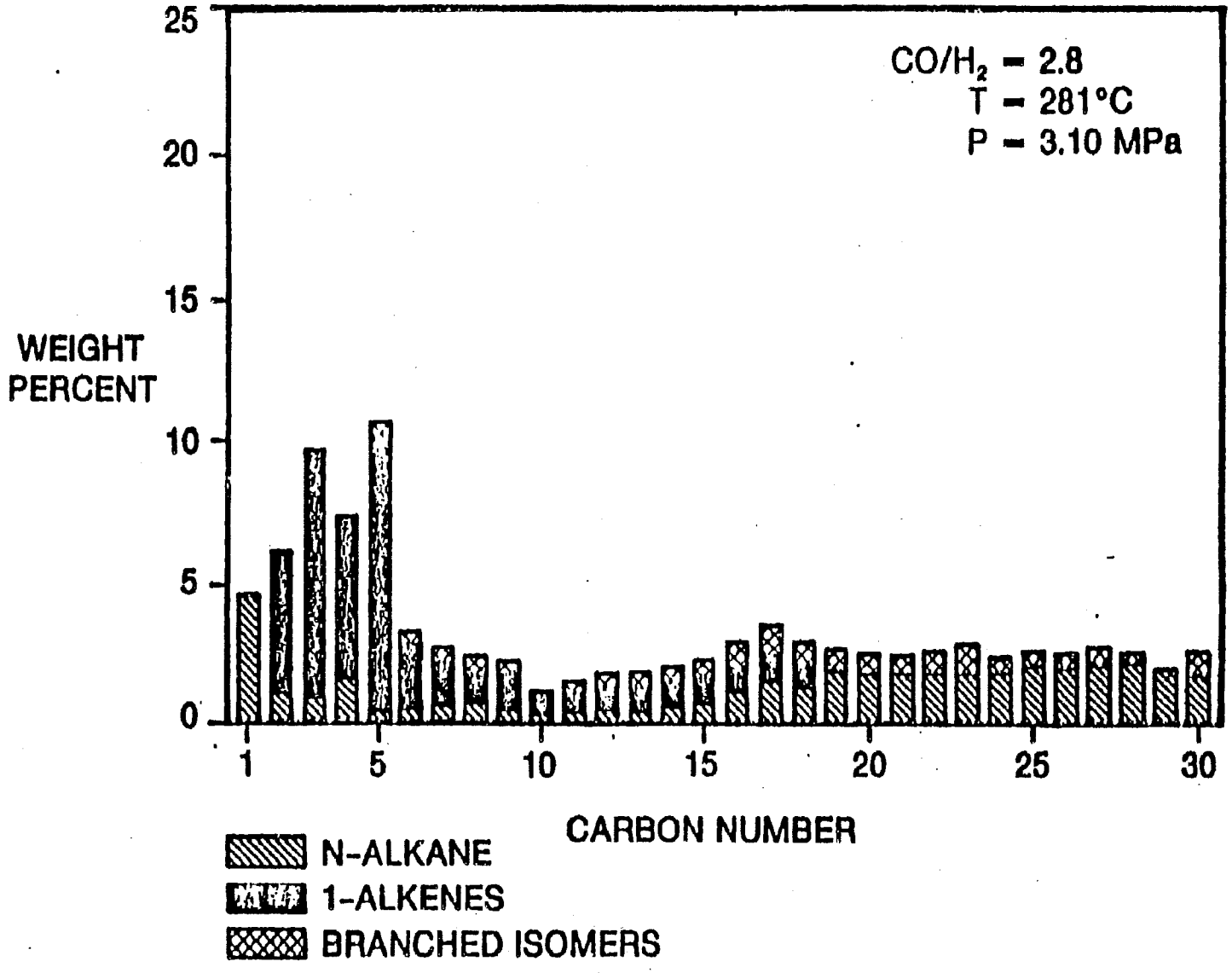

Figure 8-24. Hydrocarbon Weight Distribution for Fe_2O_3 (at 281°C, 3.10 MPa)

Reference: (74)

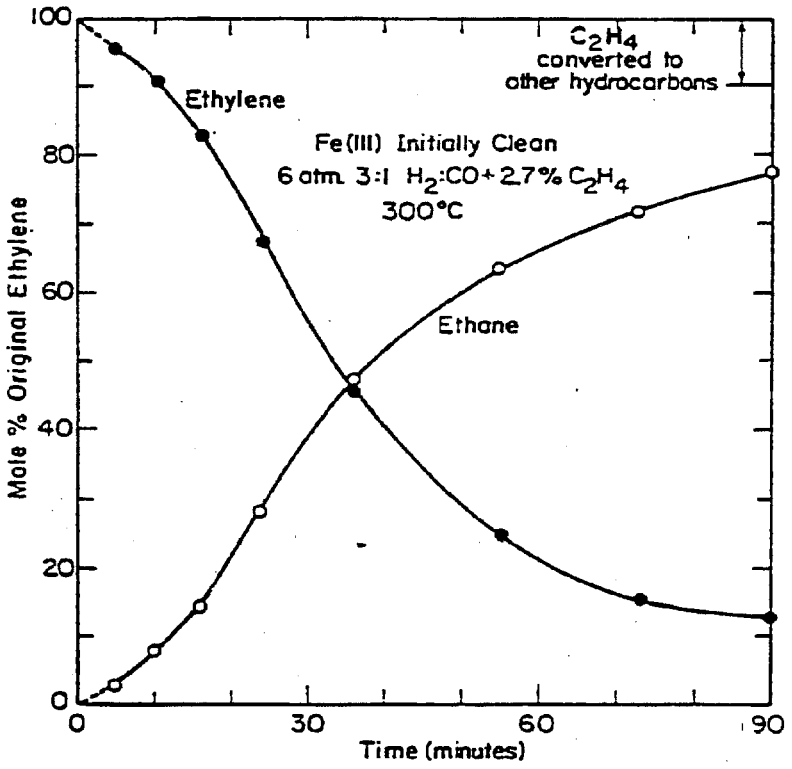

Figure 8-25. Conversion of 2.7 mol% Added Ethylene to Ethane as a Function of Time. Note that some of the ethylene is converted to other hydrocarbons

Reference: (85)

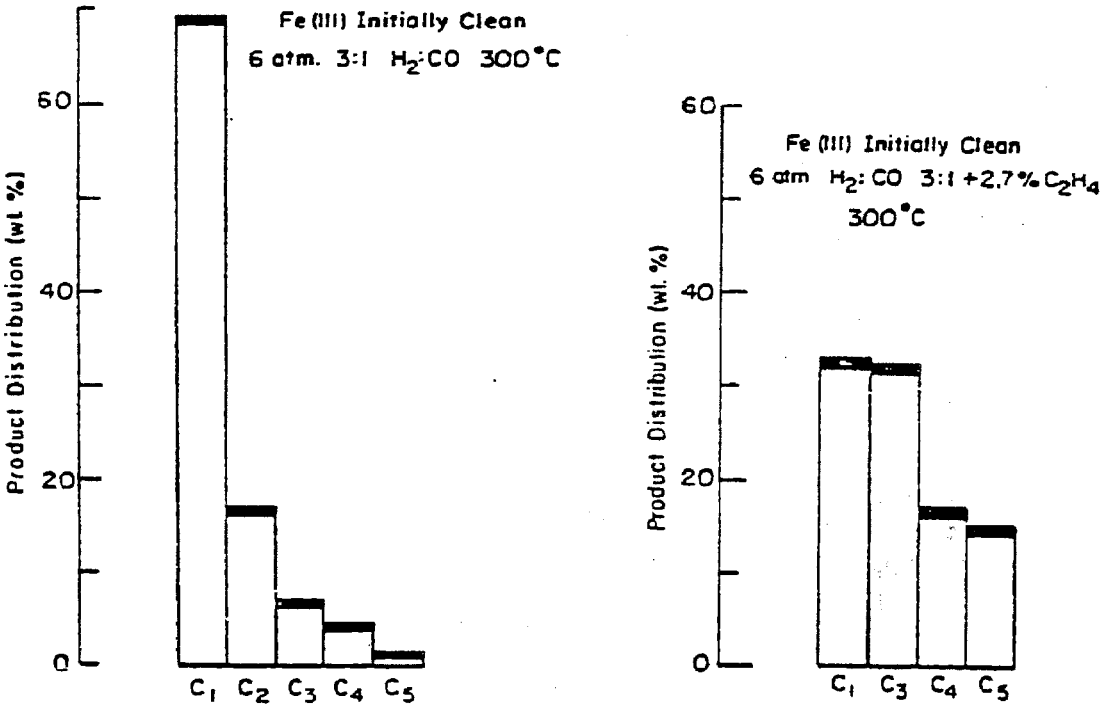

Figure 8-26. Comparison Between the Product Distribution Obtained from Initially Clean Fe^{3+} With and Without Added Ethylene. Ethylene concentration is in mol%.

Reference: (85)

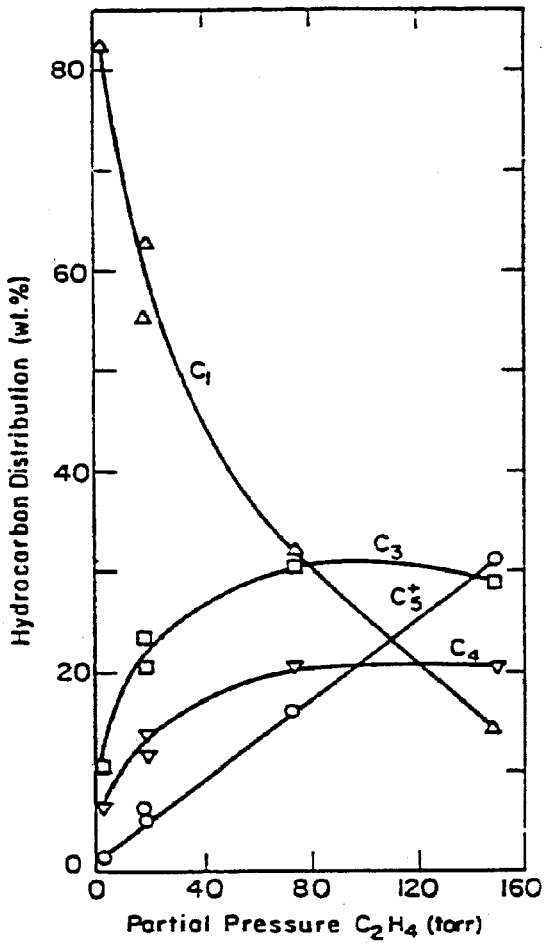

Figure 8-27. Product Distribution for Fixed Reaction Conditions (6 atm, 3:1 H_2:CO, 300°C°C as a Function of Added Ethylene

Reference: (85)

a linear correlation of C_{5+} yield with ethylene concentration, which appears to hold beyond the highest experimental value.

8.5 SUMMARY AND CONCLUSIONS

The majority of the F-T synthesis work to date can be modeled by the S-F nonselective polymerization mechanism. A striking fact about the S-F distribution is the sharp drop in the weight percent of the most abundant components as the degree of polymerization (D) increases. In fact, the distinction between the most abundant components and their neighboring components becomes less conspicuous as the value of D increases above 8. (At D = 8, the most abundant components are those with carbon numbers 7 and 8.)

There are two basic approaches to increasing the selectivity of synfuel production from syngas beyond what is possible with the S-F reactions. These are the one-step and two-step approaches. The one-step approach is a rather ambitious undertaking that is being investigated by Union Carbide, Air Products, and others. This approach is counting on a development of a multifunctional catalyst that possesses both the polymerization and shape-selective functions to produce narrow-range products. The two-step approach is represented by Mobil's methanol-to-gasoline (MTG) process. The practicality of this approach has been enhanced a great deal by the development of ZSM-5 catalysts.